NAVAL POSTGRADUATE SCHOOL
MONTEREY, CALIFORNIA

THESIS

DEVELOPMENT OF A CONTROL SYSTEM FOR A SMA ACTUATED MEDICAL MANIPULATOR

by

Richard A. Thiel

December, 1997

Thesis Advisor: Ranjan Mukherjee

Approved for public release; distribution is unlimited.

REPORT DOCUMENTATION PAGE

Form Approved
OMB No. 0704-0188

1. AGENCY USE ONLY *(Leave blank)*	2. REPORT DATE	3. REPORT TYPE AND DATES COVERED
	December 1997	Master's Thesis

4. TITLE AND SUBTITLE
DEVELOPMENT OF A CONTROL SYSTEM FOR A SMA ACTUATED MEDICAL MANIPULATOR

5. FUNDING NUMBERS
ARPA Order No. B-795
ARPA Order No. 8578
Amendment No. 9

6. AUTHOR(S)
Richard A. Thiel

7. PERFORMING ORGANIZATION NAME(S) AND ADDRESS(ES)
Naval Postgraduate School
Monterey CA 93943-5000

8. PERFORMING ORGANIZATION REPORT NUMBER

9. SPONSORING/MONITORING AGENCY NAME(S) AND ADDRESS(ES)
Advance Research Projects Agency

10. SPONSORING/MONITORING AGENCY REPORT NUMBER

11. SUPPLEMENTARY NOTES
The views expressed in this thesis are those of the author and do not reflect the official policy or position of the Department of Defense or the U.S. Government.

12a. DISTRIBUTION/AVAILABILITY STATEMENT
Approved for public release; distribution is unlimited.

12b. DISTRIBUTION CODE

13. ABSTRACT *(maximum 200 words)*

This thesis discusses the development of a digital control system for the operation of a conceptual robotic manipulator for use in minimally invasive surgery. The motion of the manipulator is envisioned to be accomplished with actuators made of Shape Memory Alloy (SMA). SMA has the ability to recover permanent deformation by undergoing a phase transformation. The recovery of the deformation results in motion of the SMA material which can be exploited for useful work. SMA was chosen as the actualtor because it can be miniturized and has a very high power density as compared to conventional actuators. An Actuator Matrix Driver (AMD) board was designed, as part of the digital control system, to power and control the SMA actuators. The matrix configuration of the AMD and the use of Amplitude Modulated Pulsed (AMP) current allows for a reduction in the number of leads for the powering and control of the actuators. The electrical resistance, a physical property of SMA which characteristically changes with phase transformation, can be used to determine the state or phase of the SMA actuators and can therefore be used for closed loop control.

14. SUBJECT TERMS
Shape Memory Alloy (SMA), Actuator Matrix Driver (AMD) Board, Amplitude Modulated Pulsed (AMP) Current

15. NUMBER OF PAGES
88

16. PRICE CODE

17. SECURITY CLASSIFICATION OF REPORT	18. SECURITY CLASSIFICATION OF THIS PAGE	19. SECURITY CLASSIFICATION OF ABSTRACT	20. LIMITATION OF ABSTRACT
Unclassified	Unclassified	Unclassified	UL

NSN 7540-01-280-5500

Standard Form 298 (Rev. 2-89)
Prescribed by ANSI Std. 239-18

298-102

Approved for public release; distribution is unlimited.

DEVELOPMENT OF A CONTROL SYSTEM FOR A SMA ACTUATED MEDICAL MANIPULATOR

Richard A. Thiel
Lieutenant Commander, United States Navy
B.S., University of Idaho, 1984

Submitted in partial fulfillment
of the requirements for the degree of

MASTER OF SCIENCE IN MECHANICAL ENGINEERING
AND
MECHANICAL ENGINEER

from the

NAVAL POSTGRADUATE SCHOOL
December 1997

Author: _____
Richard A. Thiel

Approved by: _____
Ranjan Mukherjee, Thesis Advisor

_____
Terry R, McNelley, Chairman
Department of Mechanical Engineering

ABSTRACT

This thesis discusses the development of a digital control system for the operation of a conceptual robotic manipulator for use in minimally invasive surgery. The motion of the manipulator is envisioned to be accomplished with actuators made of Shape Memory Alloy (SMA). SMA has the ability to recover permanent deformation by undergoing a phase transformation. The recovery of the deformation results in motion of the SMA material which can be exploited for useful work. SMA was chosen as the actuator because it can be miniturized and has a very high power density as compared to conventional actuators. An Actuator Matrix Driver (AMD) board was designed, as part of the digital control system, to power and control the SMA actuators. The matrix configuration of the AMD architecture and the use of Amplitude Modulated Pulsed (AMP) current allows for a reduction in the number of leads for the powering and control of the actuators. The electrical resistance, a physical property of SMA which characteristically changes with phase transformation, can be used to determine the state or phase of the SMA actuators and can therefore be used for closed loop control.

TABLE OF CONTENTS

I. INTRODUCTION

A. MOTIVATION

Laparoscopic surgery currently involves the use of rigid arms supporting surgical instruments that are inserted into the torso through a trocar. Such systems are highly constrained with respect to the maneuvers available to the surgeon. This limitation can be overcome through the development of a controllable flexible surgical manipulator.

In this research, a flexible manipulator is proposed in which very complex articulated motion can be achieved. The design stipulates that the manipulator be composed of five segments, where each segment will have three degrees of freedom. Figure 1.1 is a conceptual rendition of the flexible manipulator. The three dimensional motion capability of each segment will be provided through the use of three actuators. The actuators are to be constructed with shape memory alloy (SMA) material and a digital control system will control the motion of the actuators and consequently, of the flexible manipulator.

The manipulator's design will allow it to perform a 90° to 120° bend within a six inch radius. A force of approximately two pounds is to be resisted by the manipulator. The center space of the manipulator is to be clear, allowing for the passage of optical fibers or cables for the control of end effector. The diameter of the manipulator is limited to 10 mm or less so that the manipulator can fit through the standard size trocar currently in use.

The small diameter and hollow center space of the manipulator requires that the actuators and control system be as small as possible. This was the primary driving force for using SMA material. SMA has a very high power-to-weight ratio compared to other more conventional actuators. Also, the nature of SMA allows for the electrical resistance of the material to be used for feedback control. This allows for the integration of the powering and monitoring/control systems in to a single system, reducing the number of leads required.

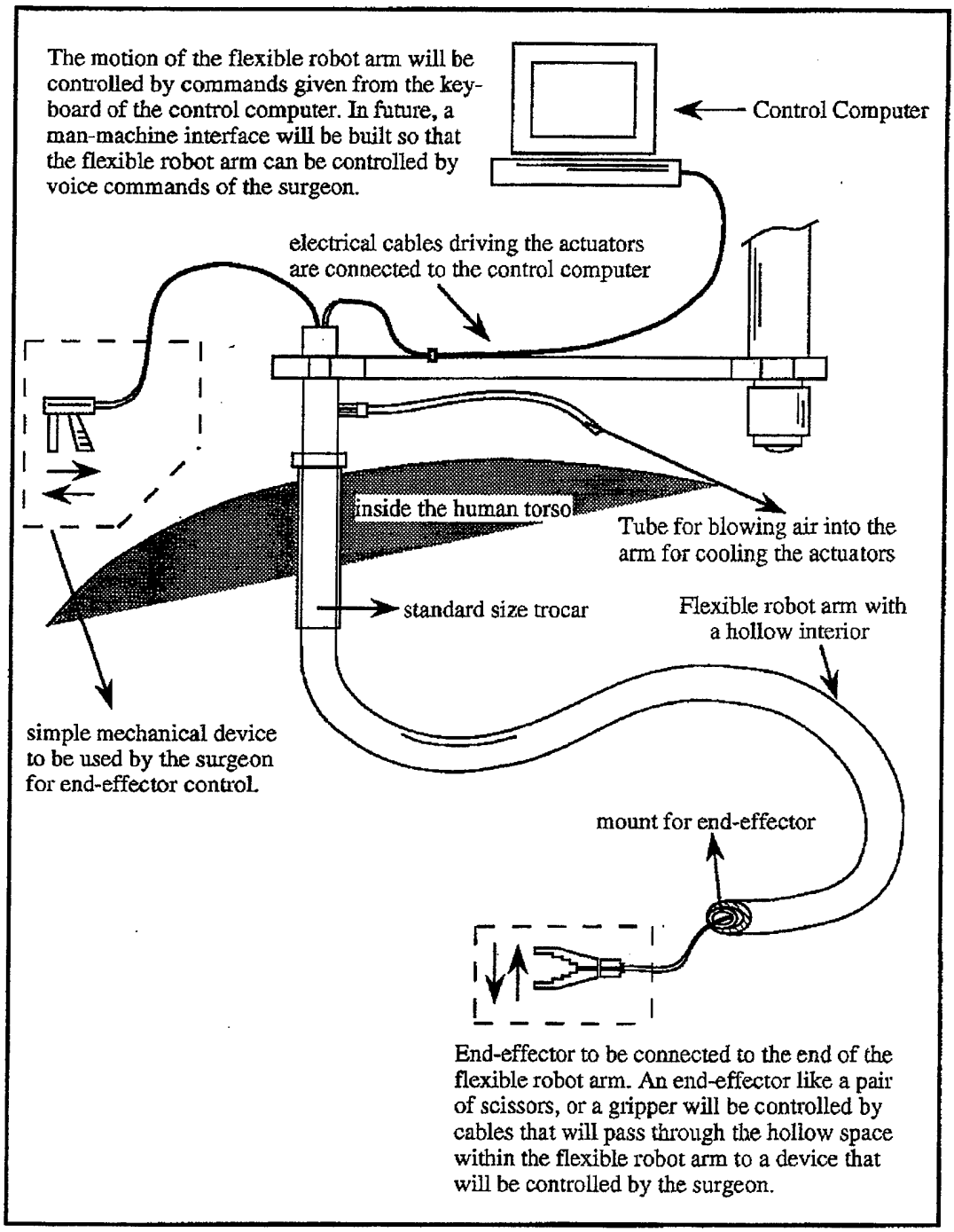

Figure 1.1: A conceptual diagram of the flexible manipulator. A gripper end effector is shown. The flexible manipulator's motion will be controlled by a digital control system with the commands being sent from the keyboard of a personal computer.

This thesis discusses the concept of thermal inertia to describe the heating and cooling characteristics of a SMA actuator wire. The concept of thermal inertia is exploited in the development of a new method of actuation and control of multiple SMA elements using a minimum number of leads. This control system addresses the SMA actuator elements sequentially by selecting a corresponding row and particular column. Using this method, each SMA actuator is sequentially powered by a pulsed current. The magnitude and duration of the pulsed current depends primarily on the environment which is cooling the SMA actuators and the maximum number of elements to be controlled during a single powering cycle. Open or closed loop control, based on electrical resistance feedback, can be used to compute the magnitude of the pulsed current once a pulse duration is determined.

B. BACKGROUND ON SHAPE MEMORY ALLOY

Shape memory alloy material has the ability to deform a relatively significant amount while the material is in its low temperature state. Heating the SMA to its phase transformation temperature causes it to recover the low temperature deformation and the material is said to "remember" it's shape before deformation [Ref. 1]. For the initial development of the control system, the SMA chosen to be used as the actuator was a wire form made of nickel-titanium, NiTi.

The mechanism for the shape memory characteristic is based on the very complex transformation of the material between martensite and austenite. The solid state transformation from austenite to martensite is displacive, athermal (time independent), first order (liberates heat), associated with a hysteresis, and occurs over a temperature span in which both phases exist. Through Bain strain and lattice invariant shear, the austenitic structure, upon cooling, is transformed into a twinned martensitic structure with little volume change. Detwinning the martensite results in a significant shape change of approximately 4 to 8 percent deformation. This deformation is fully recoverable, provided

that the applied stress level has not produced slip, when the material is heated and austenite reformed. [Ref. 1]

The NiTi actuator wire exhibits a substantial electrical resistance difference between the austenitic and martensitic phases. It is this resistance difference between the transformation phases of the SMA that the control system will exploit. A command from the control system will cause the SMA actuator to be heated by an electrical current flowing through it. Heating causes a phase change in the SMA material and leads to the

Property	English	Metric
Density	0.235 lb/in^3	6.45 gm/cm^3
Specific Heat	0.20 Btu/lb-R	6.8 cal/mol.-°C
Melting Point	2282 °F	1250 °C
Heat of Transformation	10.4 Btu/lb	24.19 kJ/kg [1]
Thermal Conductivity	10.4 BTU/hr-ft-°F	0.05 cal/sec-cm-°C
Thermal Expansion Coefficient Martensite Austenite	 3.67x10^{-6} /°F 6.11x10^{-6} /°F	 6.6x10^{-6} /°C 11.0x10^{-6} /°C
Electrical Resistivity Martensite Austenite	 421 ohms/cir mil ft 511 ohms/cir mil ft	
Linear Resistance (approx.) 0.010 inch diameter wire	 0.44 ohms/inch	 0.173 ohms/cm [1]
Transformation Temperature	129.2 °F [1]	90 °C

[1] Value calculated from figure provided by manufacturer.

Table 1.1: Nickel-Titanium alloy physical properties for Flexinol™ Actuator Wire.

recovery of deformation which results in motion. By monitoring the level of electrical resistance of the SMA actuator, the control system will be able to determine the phase of the SMA material and therefore, if deformation has been recovered.

The NiTi actuator wire was purchased from the Dynalloy Inc. located in Irvine CA. The SMA wires are marketed under the trade name of Flexinol™ Actuator Wires. The composition of the nickel and titanium is almost exactly a 50% ratio. Varying the nickel-titanium ratio slightly changes the temperature at which the SMA wire remembers its predeformed shape. Table 1.1 lists some of the physical characteristics of the SMA wire supplied from Dynalloy.

This thesis investigates the use of SMA as an actuator and is organized as follows. In Chapter II, the behavior of SMA is characterized, specifically the relationship of electrical resistance of SMA versus temperature. The heat transfer model of a SMA wire electrically heated and cooled by the environment is developed in Chapter III. The heat transfer model analysis will lead to the introduction of the concept of thermal inertia. Actual testing of a SMA wire is discussed in Chapter IV. The concept for the actuation system and the circuit description of the hardware developed for implementation of the actuation system is discussed in Chapter V. A control system developed for a set of SMA actuators is elaborated on in Chapter VI. Chapter VII is concerned with conclusions for this thesis research and with recommendations for further study.

II. SMA RESISTANCE - TEMPERATURE TESTING

The data in the literature provided by the manufacturer, Dynalloy Inc., resulted in only a sketchy incomplete view of the behavior of SMA material. The manufacturer recommended that the wire be heated electrically, but no data was provided that described the wires behavior with different current inputs. The data that was furnished was a listing for different wire diameters and an associated continuous current value. This was the continuous current which was recommended not to exceed to avoid material damage. Only one graph was provided which related the strain to the temperature of the wire. Performance of the wire was only referred to in broad generalities with the user encouraged to explore the possibilities of the SMA wire, given the general limitations of the wire, which were listed in the product literature.

The resistance data listed in the product literature was not determined by the manufacturer, but was reported from different sources not readily available.[1] An attempt was made to verify electrical resistance of the wire, but measured electrical resistance did not correspond to the data published in the product literature and repeated in Table 1.1. Accounting for changes in wire dimensions, as it was heated to phase transformation, failed to provide any further illumination on the resistance behavior discrepancy.

Two data collection experiments were used to gain a clearer understanding of SMA behavior. These experiments would determine the magnitude of the resistance change as the temperature was varied and also, would identify the temperatures at which the resistance changes occurred due to the SMA phase transformation.

The first experiment involved the SMA's resistance behavior to changes in temperature. In this experiment, the SMA wire is to be placed in a variable temperature bath. As the temperature is varied, the resistance of the SMA wire test segment is measured. The second experiment explores the behavior of a SMA wire to an applied heating electric current. Both the resistance and strain are monitored as the input current

[1] Per phone conversation with technical support personnel at Dynalloy Inc. on March, 1993.

is changed. The load placed on the wire was also varied in specific increments as the resistance and strain was monitored.

A. RESISTANCE - TEMPERATURE TEST

A test apparatus was designed to measure the resistance of an SMA wire subjected to a constant stress while the temperature was varied. Figure 2.1 is a diagram of the actual test apparatus used. The SMA wire with a constant load applied is submerged in a temperature controlled bath. A digital multimeter is used to determine the resistance of the wire as the temperature is varied.

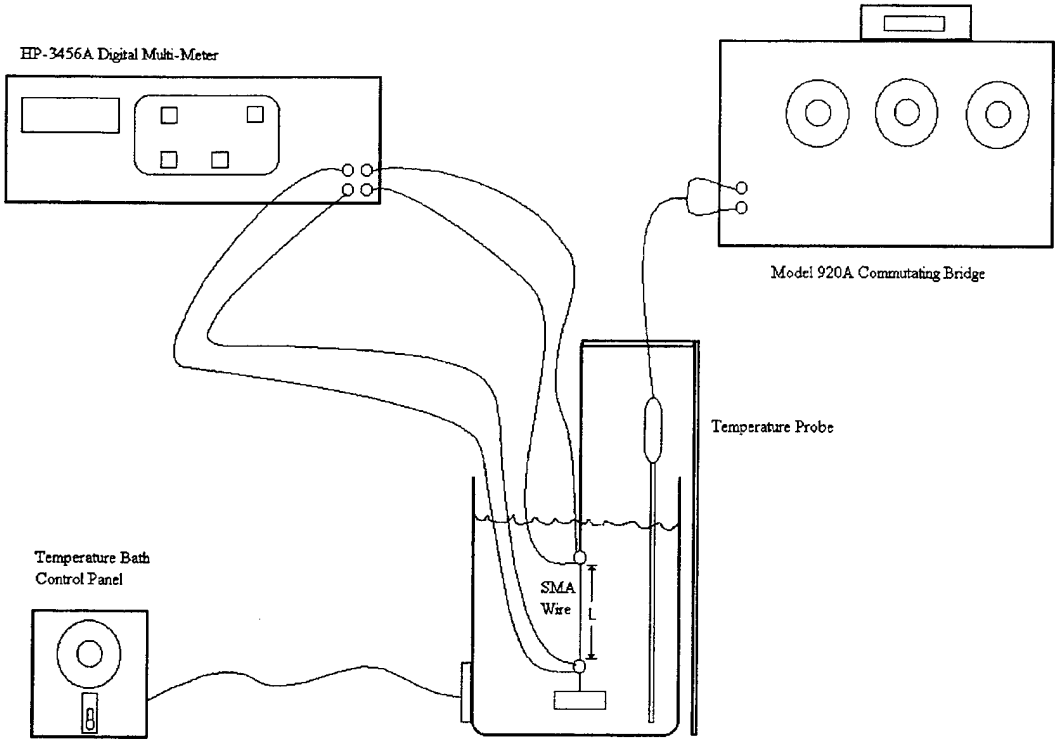

Figure 2.1: SMA Wire Resistance - Temperature Test Apparatus.

The SMA wire used for the experiment was a 0.010 inch diameter wire provided by Dynalloy. The nominal test length, L, of the SMA wire between end supports was 10.0 cm. The end supports to the SMA wire are stud ring terminal leads which were mechanically crimped to the wire. Providing the means to suspend the SMA wire in the temperature bath and to attach the applied load, the ring stud terminal leads also attached the multimeter resistance measurement leads to the SMA wire. An electrically insulated wire was used to suspend the SMA wire and weight in the bath from a table top support.

The resistance of the SMA wire was measured with a HP-3456A Digital Voltmeter manufactured by Hewlett-Packard. In the four lead resistive ohm meter mode, the digital voltmeter measures the resistance of the two high end leads and of the two low end leads. These resistance values are subtracted from the total resistance measured between the high and low leads, leaving only the measured resistance of the SMA wire.

The temperature bath system is a Model 913A Calibration Bath from the Rosemount Engineering Company (REC). The control panel consists of two dials, course and fine adjustments, for the setting of temperature of the bath. The fluid in the bath was a water and ethylene glycol mixture. Resistance of the bath fluid was in excess of 2.0 MΩ. Temperature of the bath was determined using a Platinum Resistive Thermometer (PRT). The PRT, which has NBS tracability, is immersed in the temperature bath. A Model 920A Commutating Bridge and galvanometer from REC was used to determine the resistance of the PRT. This resistance was then correlated to a specific temperature using the PRT's set of calibration tables.

B. TEST PROCEDURE

For the resistance versus temperature test of the SMA wire, a static weight was attached to the bottom end support of the wire test section. The entire assembly was then suspended in the bath. A room temperature resistance reading at no load for the wire was taken prior to starting the test. The PRT resistance, correlated bath temperature, and

SMA wire resistance were recorded at each selected temperature. Time was allowed between each set of readings for the test system to stabilize. The experiment was performed with a static weight of 341.2 gm and 234.8 gm. The SMA wire resistance recorded is the total resistance for the test wire and is not corrected due to changes in any dimensional aspect. For each data run, the temperature of the bath was increased incrementally from room temperature to approximately a temperature 20 percent greater than the stated transformation temperature of the wire. The transformation temperature, from Table 1.1, is 90 °C, therefore, the maximum temperature was approximately 108 °C. The temperature of the bath was then incrementally reduced down to room temperature.

C. RESISTANCE - TEMPERATURE TEST RESULTS

A series of resistance - temperature data runs were performed to verify the behavior of the SMA resistance as temperature was varied. Figure 2.2 is a plot of three complete resistance - temperature data runs. The plot shows extremely consistent behavior for the SMA wire resistance as the temperature is changed. From the plot, it can be seen that the resistance increases initially as the temperature is increased. At approximately 75 °C, the SMA wire begins to undergo a significant reduction in resistance. By approximately 85 °C, the resistance of the SMA wire has begun to level off and by 90 °C the resistance curve is almost flat. As the temperature is further increased, the resistance also increases.

As the temperature is lowered, the reverse trends of above are noted. The resistance decreases as the temperature is lowered until at approximately 80 °C when the resistance begins to increase. The significant increase of resistance continues as the temperature is lowered and finally levels off at approximately 57 °C. The resistance then continues to decrease as the temperature is lowered.

The sudden decrease in resistance as the temperature is increased past 75 °C is due to the start of formation of austenite. This temperature is referred to as the austenite start

temperature and labeled, T_{As}. At the point where the resistance levels off, the formation of austenite has completed. The point is called the austenite finish temperature and annotated as T_{Af}. As the temperature is reduced, formation of martensite results in the increase in resistance which starts at approximately 80 °C. T_{Ms} is the symbol used to indicate this point which is called the martensite start temperature. By 57 °C, martensite formation has completed and the resistance of the wire is what it was prior to the transformation. This point is called the martensite finish temperature, T_{Mf}.

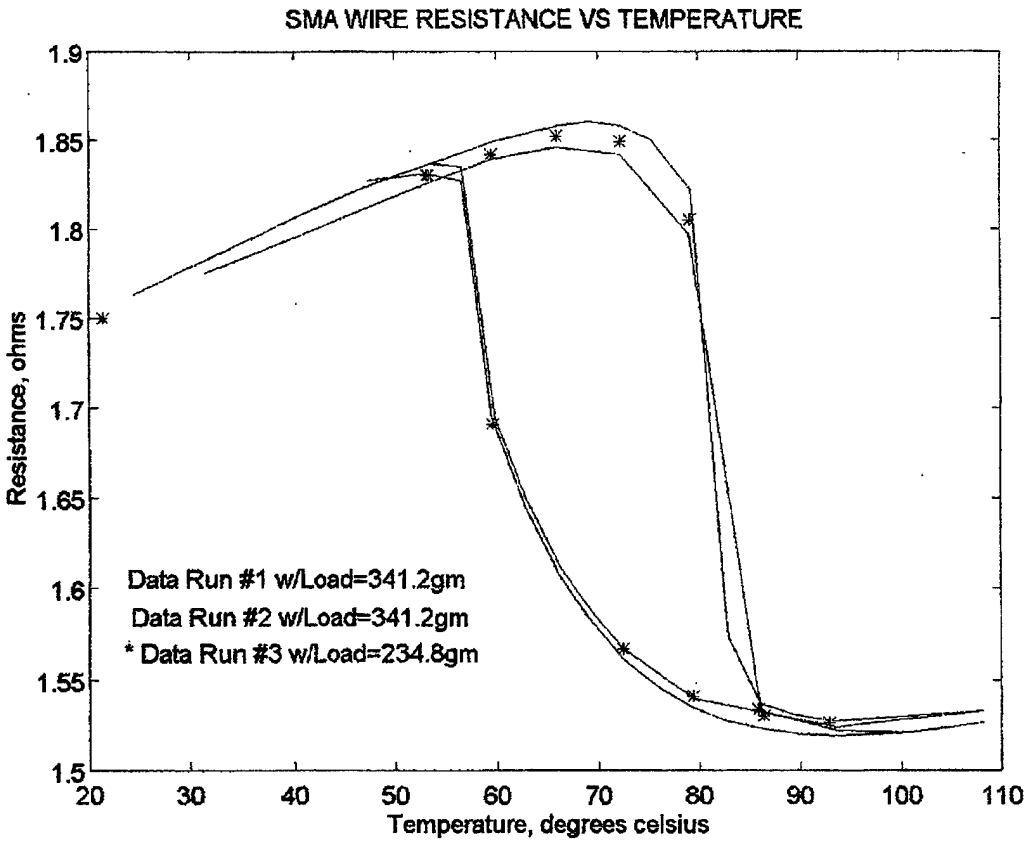

Figure 2.2: SMA Wire Resistance versus Temperature. The plot shows the SMA wire's resistance response to varying temperature for the static loads indicated. The resistance recorded is the total resistance for the nominal wire length of 10 cm ($T<T_{Mf}$).

Table 2.1 summarizes the results of the resistance - temperature test. The transformation resistance difference, ΔR, is the change in resistance measured in the wire at room temperature to the resistance at the point of transformation. This change in resistance is a roughly 11 percent decrease from the starting resistance at room temperature.

Resistance - Temperature Test Results

Point	Temperature (°C)
T_{As}	75
T_{Af}	85
T_{Ms}	80
T_{Mf}	57
Transformation ΔR	0.2 ohms

Table 2.1: Summary of Resistance - Temperature Test Results.

III. HEAT TRANSFER MODEL

After the characterization of SMA wires, the next goal was to study the mathematical model governing the heat transfer in the wire. The purpose of the model was to aid in the understanding of what was occurring with the SMA wire as it is heated and subsequently cooled during testing. Thus, the model would allow for the prediction of the wire response to an electrical driving current.

A. MODEL DESCRIPTION

A control volume was established as shown in Figure 3.1 for the heat transfer model. The dimensions of the control volume are the diameter and length of the actual SMA wire to be used for the current characteristic testing. Table 3.1 lists the control volume dimensions and also contains other terms used in the heat transfer model. The SMA wire control volume is subjected to an electrical current, the magnitude of which depends on the particular phase that is desired for the SMA. A free convection environment in ambient air is assumed to exist.

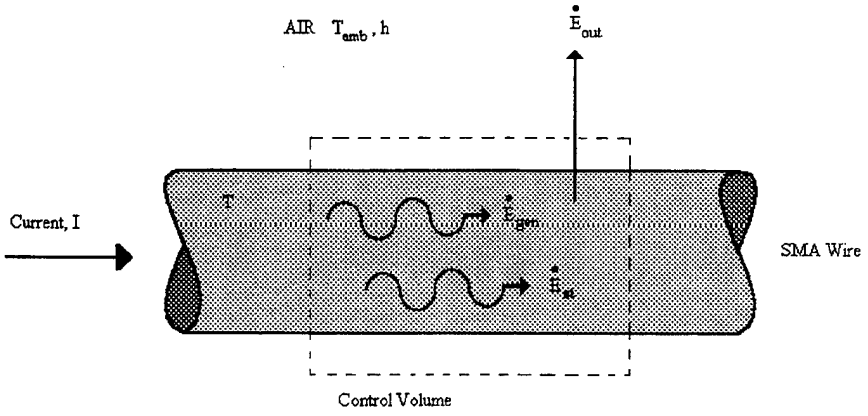

Figure 3.1: Conservation of energy for a control volume of SMA wire shown.

SMA Test Wire Heat Transfer Model Parameters		
Description	symbol	
diameter	d	0.025 cm
length (austenite)	L_a	7.184 cm
load	W	237.2 grams
% working strain	% ε	4.7 %
length (martensite)	L_m	7.522 cm
volume (martensite)	V	0.004 cm^3
surface area (martensite)	A_s	0.587 cm^2
mass	M	$2.479*10^{-5}$ kg
monitoring current	I_m	0.1 amp
heating current	I_s	2.0 amp
ambient temperature	T_{amb}	296.2 K
heat transfer coefficient	h	25 W/m^2* K

Table 3.1: List of test wire parameters for the Heat Transfer Model.

Figure 3.1 shows all the possible energy terms that may be considered for the heat transfer model. Appendix A: Heat Transfer Model Calculations Using MATHCAD™ contains the calculations performed for the heat transfer modeling.

B. HEAT TRANSFER MODEL EVALUATION[2]

1. Phase 1: Monitoring of SMA Wire with Monitoring Current, I_m

In the initial phase, the SMA wire is subjected to only a monitoring current, I_m, as listed in Table 3.1. This current is used to determine the resistance value of the wire before it is heated with current Is. Due to the SMA wire's electrical resistance, the monitoring current results in the generation of thermal energy inside the control volume. It is desired to know the wire temperature due to the energy generation.

The first law of thermodynamics is applied to the SMA wire control volume. The wire is assumed to be in a thermodynamic steady state condition, thus the energy storage term, E_{st}, shown in Figure 3.1 is equal to 0. Therefore, the rate of thermal energy generation equals the rate of energy leaving the control volume:

$$\dot{E}_g = \dot{E}_{out} \tag{3.1}$$

where the rate of thermal energy generation is a result of the electrical resistance heating:

$$\dot{E}_g = I^2 \times \Omega_m \times L_m \tag{3.2}$$

and the rate of energy out is due to the convective heat transfer from the surface of the SMA wire:

$$\dot{E}_{out} = h \times A_s \times (T_i - T_{amb}) \tag{3.3}$$

Substituting Equations 3.2 and 3.3 into 3.1:

$$I^2 \times \Omega_m \times L_m = h \times A_s \times (T_i - T_{amb}) \tag{3.4}$$

---

[2] Evaluation of the heat transfer model was performed utilizing Reference 3.

From Equation 3.4, the equilibrium temperature of the SMA wire can be determined:

$$T_i = \frac{I^2 \times \Omega_m \times L_m}{h \times A_s} + T_{amb} \tag{3.5}$$

substituting in heat transfer model Table 1.1 values:

$$T_i = \frac{(0.1 \cdot amp)^2 \times (0.173 \cdot \frac{ohm}{cm}) \times (7.522 \cdot cm)}{\left(25 \cdot \frac{W}{m^2 \cdot K}\right) \times (0.587 \cdot cm^2)} + (296.2 \cdot K)$$

$$T_i = 304.88 \cdot K$$

2. Phase 2: Heating of SMA Wire with Input Current, I_s

During this phase, the SMA wire is subjected to a short duration step pulse current of I_s. This current is used to heat the martensitic wire to its transformation temperature of austenite start, T_{As}, and then to supply the energy necessary to complete the transformation at the austenite finish temperature, T_{Af}. The short duration of the applied current allows for the heat transfer out of the control volume, E_{out} as shown in Figure 3.1, to be neglected.

From the first law, the thermal energy generation will increase the internal energy of control volume. The increase in internal energy will first heat the wire to the point of transformation and then cause the desired phase transformation:

$$E_g = \Delta E_{st} = E_h + E_t \tag{3.6}$$

where the energy required to heat the wire to the point of transformation:

$$E_h = \rho \times V \times C_p \times (T_{As} - T_i) \tag{3.7}$$

and the energy required for the phase transformation:

$$E_t = M \times h_t \tag{3.8}$$

The thermal energy generation is equal to Equation 3.2 over a time period Δt:

$$E_g = I^2 \times \Omega_m \times L_m \times \Delta t \tag{3.9}$$

In order to determine the time necessary to heat the wire to the point of transformation, consider Equations 3.7 and 3.9, solving for the time period, Δt_h:

$$\Delta t_h = \frac{\rho \times V \times C_p \times (T_{As} - T_i)}{I^2 \times \Omega_m \times L_m} \tag{3.10}$$

substituting in heat transfer model Table 1.1 values:

$$\Delta t_h = \frac{(6.505 \cdot \frac{gm}{cm3}) \times (0.004 \cdot cm3) \times (0.2 \cdot \frac{cal}{gm \cdot K}) \times ((343 - 304.88)K)}{(2 \cdot amp)^2 \times (0.173 \cdot \frac{ohm}{cm}) \times (7.522 \cdot cm)}$$

$$\Delta t_h = 0.152 \cdot \text{sec}$$

From this point, the thermal energy generated is equal to the energy needed for the phase transformation. Combining Equations 3.8 and 3.9, the time for the phase transformation can be calculated:

$$\Delta t_t = \frac{M \times h_t}{I^2 \times \Omega_m \times L_m} \tag{3.11}$$

substituting in heat transfer model Table 1.1 values:

$$\Delta t_t = \frac{(2.479 \bullet 10^{-5} \cdot kg) \times (24.19 \cdot \frac{kJ}{kg})}{(2 \cdot amp)^2 \times (0.173 \cdot \frac{ohm}{cm}) \times (7.522 \cdot cm)}$$

$$\Delta t_t = 0.115 \cdot \text{sec}$$

Therefore, the total time required to heat the SMA wire to complete phase transformation is:

$$\Delta t = \Delta t_h + \Delta t_t = 0.267 \cdot \text{sec}$$

3. Phase 3: Cooling of the SMA Wire

The final phase of the wire characterization test involves the cooling of the SMA wire while monitoring the resistance as it undergoes the phase transformation from austenite to martensite. Of particular concern is the length of time that is required for the temperature of the wire to decay from the austenite finish temperature, T_{Af}, to the martensite start temperature, T_{Ms}. The time calculated is a maximum limit of concern, as will be discussed later. Therefore, neglecting the relatively low monitoring current of 0.1 amp will generate a small error to the conservative direction; the true decay time will be longer than the calculations will show.

Using the conservation of energy for the control volume of Figure 3.1, the rate of energy flow out results in an equal rate of decrease in energy storage:

$$-\dot{E}_{out} = \dot{E}_{st} \tag{3.12}$$

To simplify the model, an assumption is made that the temperature in the wire is uniformly distributed throughout at any particular time as the wire is cooling. This assumption is the basis of the lumped capacitance method which relies on the requirement that the material have minimal temperature gradients. See Appendix A for the justification to use the lumped capacitance method for evaluation. Equation 3.12 is expressed in its differential equation form of:

$$-h \times A_s \times (T - T_{amb}) = \rho \times V \times C_p \times \frac{dT}{dt} \tag{3.13}$$

An expression is substituted for the temperature difference term to simplify the integration:

$$\theta = T - T_{amb} \quad \text{and then} \quad \frac{d\theta}{dt} = \frac{dT}{dt} \tag{3.14 a \& b}$$

substituting Equation 3.14 a & b into Equation 3.13:

$$-h \times A_s \times \theta = \rho \times V \times C_p \times \frac{d\theta}{dt} \tag{3.15}$$

Rearranging and integrating, see Appendix A, Equation 3.15 results in the expression for the transient temperature response:

$$\frac{\theta}{\theta_i} = \frac{(T - T_{amb})}{(T_i - T_{amb})} = \exp[-(\frac{h \times A_s}{\rho \times V \times C_p}) \times t] \tag{3.16}$$

Two common substitutions can be made for the term inside the exponential operator. The first is the resistance to convective heat transfer, R_t:

$$R_t = \frac{1}{h \times A_s} \tag{3.17}$$

and the second is the lumped thermal capacitance, C_t:

$$C_t = \rho \times V \times C_p \tag{3.18}$$

Combining Equations 3.17 and 3.18 and simplifying yields the expression for the thermal time constant, τ_t:

$$\tau_t = R_t \times C_t \tag{3.19}$$

using the expressions for Equations 3.17 and 3.18:

$$\tau_t = \left(\frac{1}{h \times A_s}\right) \times (\rho \times V \times C_p) \tag{3.20}$$

substituting in heat transfer model Table 1.1 values:

$$\tau_t = \frac{(6.505 \cdot \frac{gm}{cm3}) \times (0.004 \cdot cm3) \times (0.2 \cdot \frac{cal}{gm \cdot K})}{\left(25 \cdot \frac{W}{m^2 \cdot K}\right) \times (0.587 \cdot cm^2)}$$

$$\tau_t = 13.835 \cdot \text{sec}$$

which is the time required for the temperature of the wire to decay to 0.368 its original value. Substituting Equation 3.17, 3.18, and 3.19 into 3.16 and solving for the temperature of the wire results in:

$$T = T_{amb} + \theta_i \times \exp\left(\frac{t}{\tau_t}\right) \tag{3.21}$$

where

$$\theta_i = T_i - T_{amb} \qquad (3.21\ a)$$

See Figure 3.2 for a plot of Equation 3.20, the transient temperature response of SMA wire undergoing free convection cooling. [Ref. 3]

The length of time required for the SMA wire temperature to decay from T_{Af} to T_{Ms} can be determined by solving Equation 3.21 for time , t, and substituting T_{Af} for T_i and T_{Ms} for T:

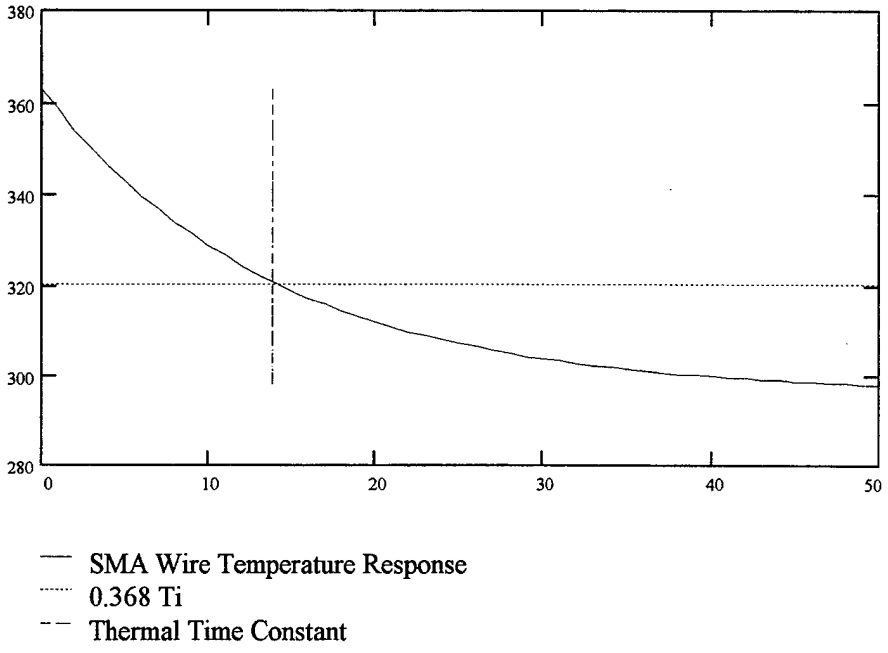

Figure 3.2: Transient temperature response of SMA wire undergoing free convection cooling. Lumped capacitance method used to evaluate the transient temperature response of the SMA wire.

$$t = \tau_t \times \ln(\frac{T_{Ms} - T_{amb}}{\theta_i}) \tag{3.22}$$

where

$$\theta_i = T_{Af} - T_{amb} \tag{3.22 a}$$

substituting in heat transfer model Table 1.1 values:

$$t = (13.8835 \cdot \text{sec}) \times \ln(\frac{353 \cdot K - 296.2 \cdot K}{363 \cdot K - 296.2 \cdot K}) = 2.244 \cdot \text{sec}$$

The time required for the SMA wire to decay from the austenite finish temperature to the martensite start temperature is 2.244 seconds. This is 8.4 times longer than the total time required to heat the wire and 19.5 times longer than the time required for transformation.

C. THERMAL INERTIA

From the above analysis, it can be seen that there is a significant time difference between the heating phase and the initial cooling phase from the austenite finish temperature down to the martensite start temperature. The time required to heat the wire is very short compared to the time experienced by the wire for the temperature to decay to the start of reverse transformation. For the action of causing the wire to contract and maintain this condition, this is a favorable predicted time difference. The time difference or delay can be referred to as the "thermal inertia" of the system. The SMA wire should exhibit a delay in reverse phase transformation not only due to the hysteresis behavior of the SMA material, but also due to the nature of convective heat transfer. The above analysis has shown that the heating phase time is a function of the input current, I_s, while the cooling time is a function of the convective heat transfer conditions. Similar analysis would show that doubling input currents would shorten the heating phase time by 50

percent while the cooling time would remain constant provided the convective heat transfer conditions did not change.

Further manipulation of Equation 3.16 yields an expression for the energy loss due to convective heat transfer for a known time period:

$$E_L = \rho \times V \times C_p \times \theta_i \times [1 - \exp(\frac{t}{\tau_t})] \tag{3.23}$$

where

$$\theta i = (T_{Af} - T_{amb}) \tag{3.23 a}$$

Substituting in the time to the point of reverse transformation calculated using Equation 3.22, the total energy loss to the point of transformation is:

$$E_L = (6.505 \cdot \frac{gm}{cm^3}) \times (0.004 \cdot cm^3) \times (0.2 \cdot \frac{cal}{gm \cdot K}) \times (363 - 296.2) \cdot K \ldots$$

$$\ldots \times [1 - \exp(\frac{2.244 \cdot \sec}{13.835 \cdot \sec})]$$

$$E_L = 0.203 \cdot joules$$

This energy loss, E_L , can then be substituted into Equation 3.10 to yield the time needed to reheat the SMA wire to the austenite finish temperature:

$$\Delta t_{rh} = \frac{E_L}{I^2 \times \Omega_m \times L_m} \tag{3.24}$$

For the heat transfer model investigated, substituting in heat transfer model Table 1.1 values:

$$\Delta t_{rh} = \frac{0.203 \cdot joules}{(2 \cdot amp)^2 \times (0.173 \cdot \frac{ohm}{cm}) \times (7.522 \cdot cm)}$$

$$\Delta t_{rh} = 0.041 \cdot \text{sec}$$

Or if a cycle time span is known, Equation 3.16 can be solved for the current needed to reheat the SMA wire to the T_{Af} temperature:

$$I_{rh} = \sqrt{\frac{E_L}{\Delta t_{rh} \times \Omega_m \times L_a}} \tag{3.25}$$

substituting in heat transfer model Table 1.1 values, energy loss E_L and assuming a reheat cycle time of Dt_{rh} = 0.267 sec:

$$I_{rh} = \sqrt{\frac{0.203 \cdot joules}{(0.267 \cdot \text{sec}) \times (0.173 \cdot \frac{ohm}{cm}) \times (7.522 \cdot cm)}}$$

$$I_{rh} = 0.76 \cdot amp$$

The above evaluation indicates that due to the heat transfer behavior of the SMA wire, considerably less heating time is required for maintaining the wire in the austenite region, if the current remains constant. Alternately, for a given reheat cycle time, the current is less than required to heat the wire.

IV. SMA RESPONSE TO AN ELECTRIC HEATING CURRENT

The heat transfer model provides an expected behavior for the SMA actuators or test elements. The next step was to electrically heat the wire and measure the changes in resistance and strain to establish the actual behavior of the SMA wire test element. Once this behavior is determined, a control system can be persued. The testing that was performed involved applying a heating electric current to a SMA test wire under a constant and varying load while measuring the change in wire length and resistance.

A. RESISTANCE / STRAIN - CURRENT TESTING

A test apparatus was designed to measure the resistance and motion of a SMA wire test element. Figure 4.1 is a diagram of the actual test apparatus used. A SMA test wire is positioned within the SMA Wire Test Stand. The test stand allows for a constant load to be applied to the SMA wire and for the motion of the wire to measured. Current is passed through the SMA wire and a resistor in series with the wire. A probe and associated target allow for the contraction of the SMA wire to be measured. The potential drop across a known resistor is measured and using ohm's law, the current through the resistor and therefore the SMA wire is determined. The voltage drop across the SMA wire is measured and together with the current is used to calculate the resistance of the wire. A function generator is used to control the output of the dc power supply which provides the current to the wire. A personal computer with a data acquisition card is used to record and process the data from the test.

The SMA Wire Test Stand was designed for the specific purpose of testing the wire's electrical resistance and strain response to an electric current input. It was built at the Naval Post Graduate School Mechanical Engineering machine shop. The stand is constructed almost exclusively of aluminum components. A one inch thick plate, 29 x 8 inches, forms the stand foundation. A 12 inch high U frame is the upper support for the

SMA test wire. The U frame legs are one inch diameter aluminum bars and the cross member is a one inch square bar that is 6.5 inches long. Through a hole drilled in the center of the cross member is a J hook welded to a threaded bar. The J hook - threaded bar holds the SMA test wire in position below the U frame cross member.

The lower end of the test wire is connected to a cantilever beam via a double J hook assembly made up through the beam. The opposite J hook below the beam is the support for an eye bolt use to hang threaded brass weights. The weights provide a steady constant load applied on the SMA test wire. The fixed end of the cantilever beam is set in a three inch square by six inch high column. The free distance between the column and the SMA wire is 12 inches. A plain carbon steel target is mounted at the end of the cantilever beam.

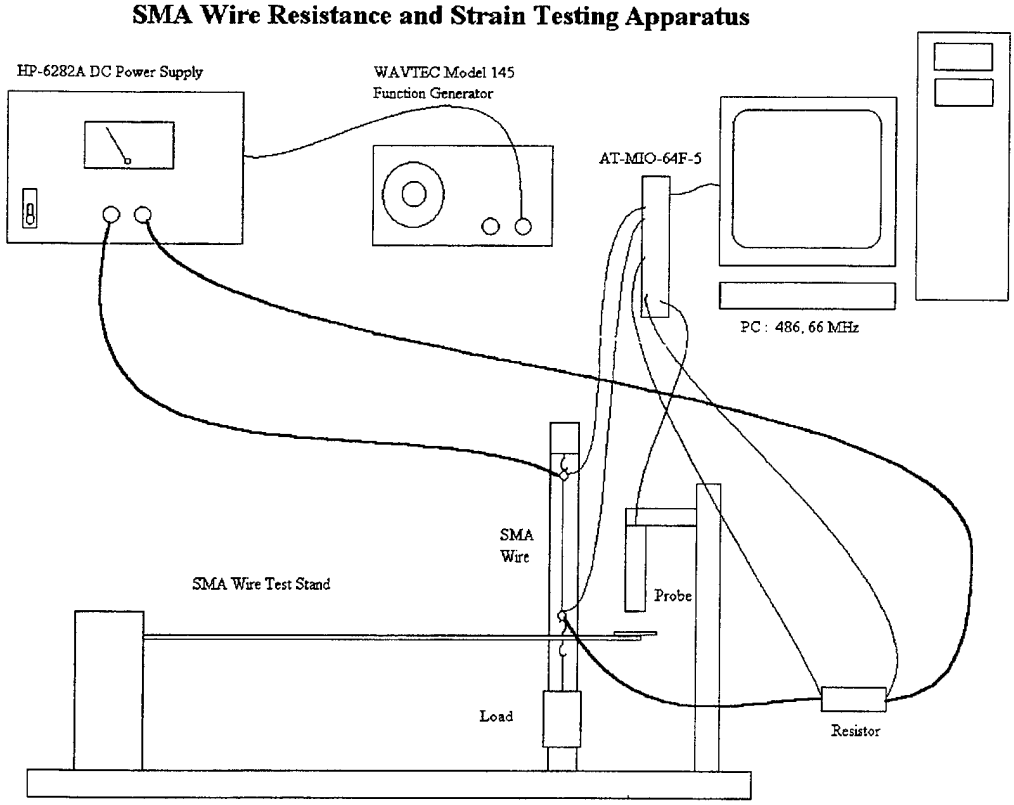

Figure 4.1 : SMA Resistance/Strain - Current Test Apparatus.

To determine the deflection of the SMA test wire, an Electro-Mike® electromagnetic displacement transducer, Model PA11503, was used to measure the target motion. A full scale reading of 10.00 volts occurs when the target is 0.500 inches from the transducer. Zero scale occurs at a target to transducer distance of 0.050 inches and a 1.000 volt output. The upper threaded J hook allows for the SMA wire to be adjusted so that its motion is within the transducers range of operation.

A resistor was wired in series with the SMA test wire. The resistance of the resistor is precisely known at 0.487 ohms and a variance of less than 1 percent up to the rated power of 30 watts. By measuring the voltage drop across the resistor, the current flow can be calculated. The resistor is in series with the SMA wire and, therefore the same current flows through both elements.

The current is supplied by a HP-6282A DC Power Supply manufactured by Hewlett-Packard. The power supply is rated for 0-10 volts at 0-10 amps and has a transient recovery time of less than 50 msec for an output recovery to within 15 millivolts following a current change in the output equal to the current rating of the supply or 5 amperes, whichever is smaller. Remote programming of the power supply output can be performed using resistance of voltage as the programming device. Remote programming can be done in both the output modes of constant current and constant voltage. For the tests conducted, the power supply was used in the remote programming mode for constant current output using voltage as the programming device. In this mode, the current output is set by the programming voltage and the voltage output is allowed to vary to maintain this output current. [Ref. 4]

The programming voltage was provided by a function generator manufactured by WAVETEK. Model 145 is a 20 MHz Pulse/Function Generator. The output of the function generator was used to program the output current of the power supply and to trigger data acquisition. The function generator can continuously generate an output signal or it can operate in a remote trigger or manual trigger mode.

Data acquisition was performed by an IBM compatible personal computer (PC) with an analog and digital I/O data acquisition board installed. The PC system consists of a 80486-66MHz DX2 ISA mother board including an Intel 80486 processor with an integrated enhanced numeric coprocessor, 32-bit local bus, 16 MB of RAM, and a 540 MB hard disk. The data acquisition board is a National Instruments® AT-MIO-64F-5 multifunction I/O board which features: 12-bit ADC, 200 kHz sampling rate, up to 64 analog inputs, 8 digital I/O , and two 12-bit DACs with voltage outputs.

B. TEST PROCEDURE

A series of tests were conducted to determine the behavior of a SMA wire to an electric heating current. As the wire is heated by, for example, a step function electric heating current, the resistance and the strain will be calculated, recorded, and plotted.

The WAVETEK function generator was operated in the manual trigger mode, therefore no signal was generated until it was manually triggered using the switch on the front panel. The signal function shape chosen was a triangle and a step, both with a DC offset. The DC offset programming voltage was such that the level of pre- and post-heating current was 0.1 ampere. This current allowed for the determination of the SMA wire resistance while minimally heating the wire. The signal function programming voltage was such that the maximum heating current was approximately 1.0 amp. This current was the manufactures recommended maximum continuous current for the 0.010 " diameter SMA wire so that overheating did not occur. Both the signal function and DC offset selections were performed with the dials on the front of the function generator panel. The duration of the heating cycle was varied by adjusting the frequency/period dial on the front panel of the function generator.

The data recorded for each test sequence was the voltage output of the DC power supply, the voltage drop across the SMA test wire, voltage drop across the resistor, and the transducer voltage. Data acquisition was conducted using the computer programming

software LabVIEW®. A more detailed description of this programming software is included in Chapter VI SMA ACTUATOR CONTROL SYSTEM.

A LabVIEW® program titled "SMA wire test - SE Trig.vi" configures the National Instruments® data acquisition board, specifies the number of scans of data points to record, the scan rate, channels to access and record, the trigger channel, number of pretrigger scans, and a file to write the data to. The program also displays the data collected and has the option of not saving the data collected. A copy of the software front panel and the diagram of the program are shown in Appendix B.

The data collected using the LabVIEW® program "SMA wire test - SW Trig.vi" was written to a file on the PC system hard disk. The software program MATLAB® [Ref. 4] was used to analyze and process the data and calculated the SMA test wire's resistance and strain. The series resistor data was used to calculate the current passing through the SMA test wire. This was then used with the data collected for the voltage drop across the SMA test wire to determine the SMA wires resistance. MATLAB® was then used to generate two sets of plots. The first plot is of the three curves of electric heating current, SMA test wire strain and resistance versus time and the second plot is of the SMA test wire resistance versus time.

C. RESISTANCE / STRAIN - CURRENT TEST RESULTS

Two different series of tests were performed on a SMA wire test segment. The first series of tests involved a fixed heating current with a fixed heating cycle time. The second series of tests pertained to a SMA wire with a fixed static weight and a constant heating current while the heating cycle time is varied. Then, the last set of tests was conducted with the heating cycle time fixed while the current is varied.

As stated above, the LabVIEW® program "SMA wire test - SW Trig.vi" was used to configure the National Instruments® data acquisition board. The number of scans was 2250 scans, scan rate was 150 scans/sec, and the number of pretrigger scans was 75 scans.

This combination resulted in a test duration of 15 seconds of data with 0.5 seconds being of pre-trigger data. The trigger was set to the DC power supply voltage increasing positively past 0.4 volts. Table 4.1 summarizes the program test parameters.

For both sets of tests, the SMA test wire were in a relatively still air environment. Therefore, a free convective situation was assumed to exits but with an aggressive convective heat transfer coefficient. Reference 3 provided guidance on convective heat transfer coefficient values.

Program Test Parameters

number of scans	2250 scans
scan rate	150 scans/sec
pretrigger scans	75 scans
test duration	15 seconds
pretrigger time	0.5 seconds
trigger source	DC Power Supply
trigger level	0.4 volts
trigger slope	rising

Table 4.1: LabView program test parameters for collecting SMA wire test data.

1. Variable Load Testing

For the first series of tests, four different loads were used. The loads consisted of beam only (no weight), 130.6 gm, 237.2 gm, and 344.2 gm. The parameters are summarized and listed in Table 4.2 for the variable load tests of the SMA test wire. Two plots, 1) current, resistance, and strain versus time and 2) resistance versus time, were generated for each data run using MATLAB® and are shown in Figures 4.2 through 4.5. The function generator was set to output a programming voltage signal in the shape of a triangle function. The voltage signal had a heating cycle lasting for 5 seconds and the off or monitoring cycle lasting for the remaining portion of the test duration, 10 seconds.

Review of Figures 4.2 through 4.5 shows that the heating and monitoring cycles are practically identical. The strain experienced by the wire increases as the static load on the wire increases. This behavior is related to the different mechanical properties of austenite and martensite. For NiTi alloys, Young's Modulus of Elasticity increases from martensite to austenite [Ref. 6 and 7]. Because of this difference in mechanical behavior, more strain is recovered when the SMA wire is heated at higher stress levels.

Table 4.2 also shows that the resistance of the SMA wire is independent of the stress or load placed on the wire. The austenite and martensite resistance of the SMA wire is constant and independent of stress level. Thus, resistance monitoring will not reveal the extent of recovered strain in the SMA wire. Resistance monitoring will only indicate the phase of the SMA.

Variable Load Test

wire length (austenite) : 8.13 cm				
ambient temperature : 23.0 °C				
load	% strain	Ω, austenite	Ω, martensite	% Ω change
beam only	0.71	1.24	1.41	12.06
130.6 gm	2.19	1.25	1.42	11.97
237.2 gm	4.4	1.25	1.41	11.35
344.2 gm	5.08	1.25	1.43	12.59

Table 4.2 : Variable Weight Test. Test parameters and results for the variable weight testing of the SMA test wire.

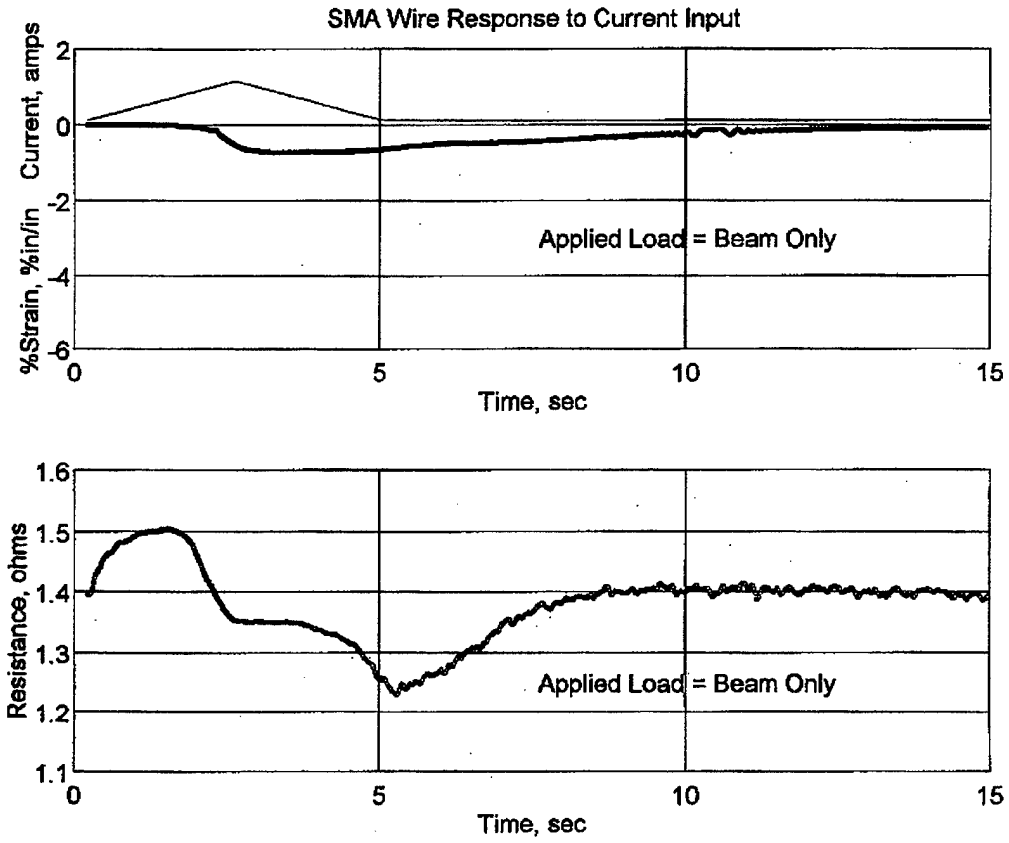

Figure 4.2 : Variable Load Test, Beam only.

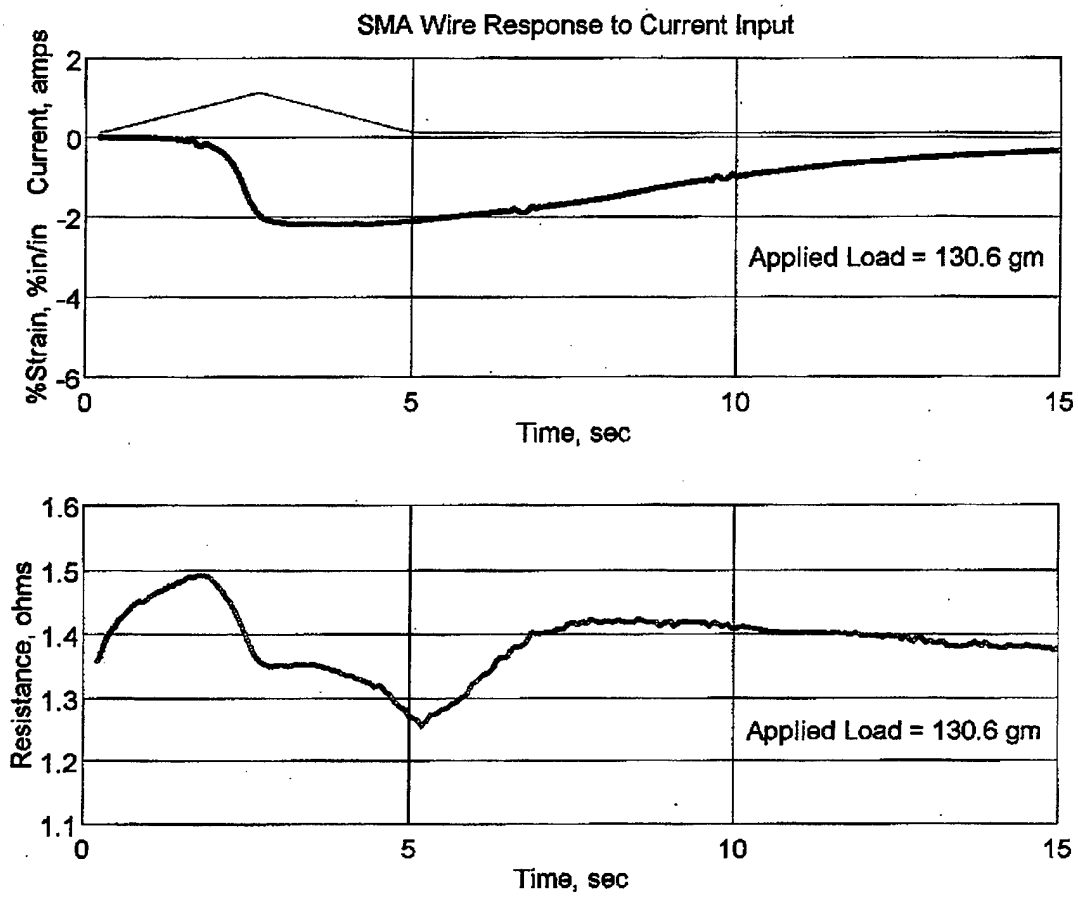

Figure 4.3 : Variable Load Test, 130.6 gm.

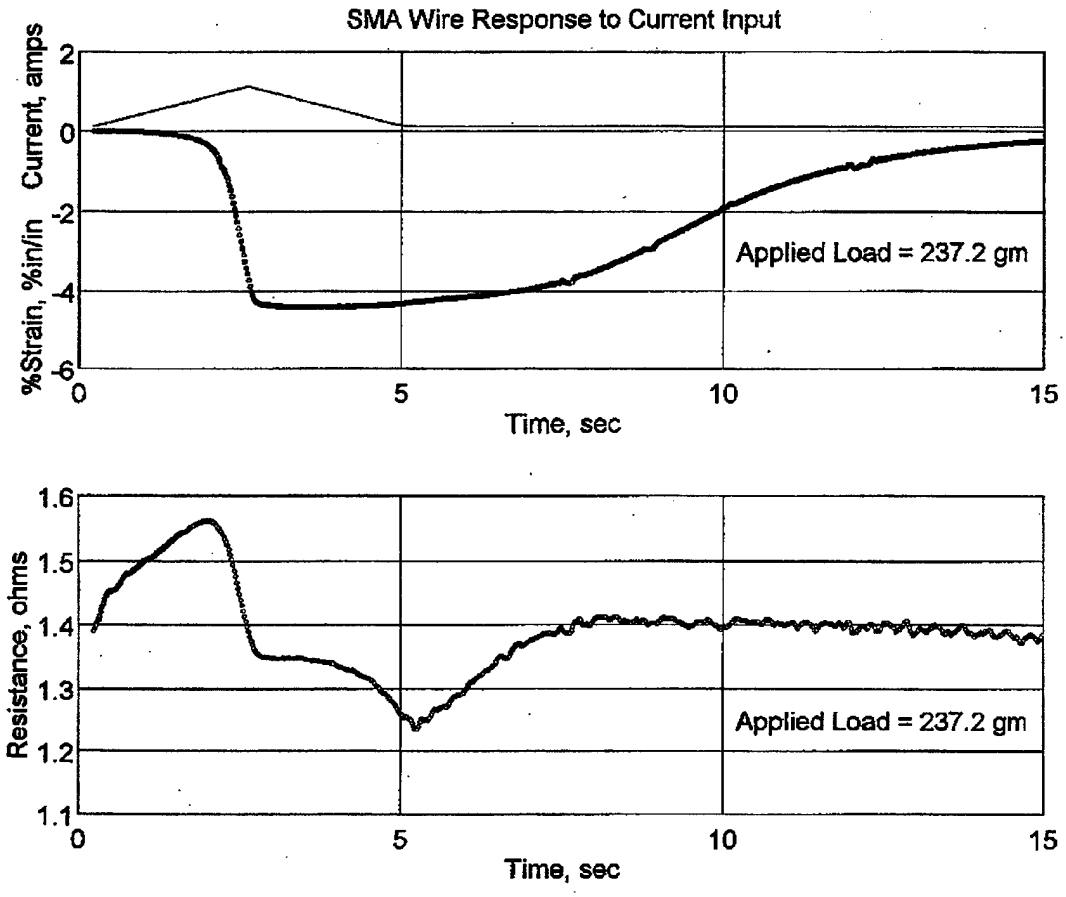

Figure 4.4 : Variable Load Test, 237.2 gm.

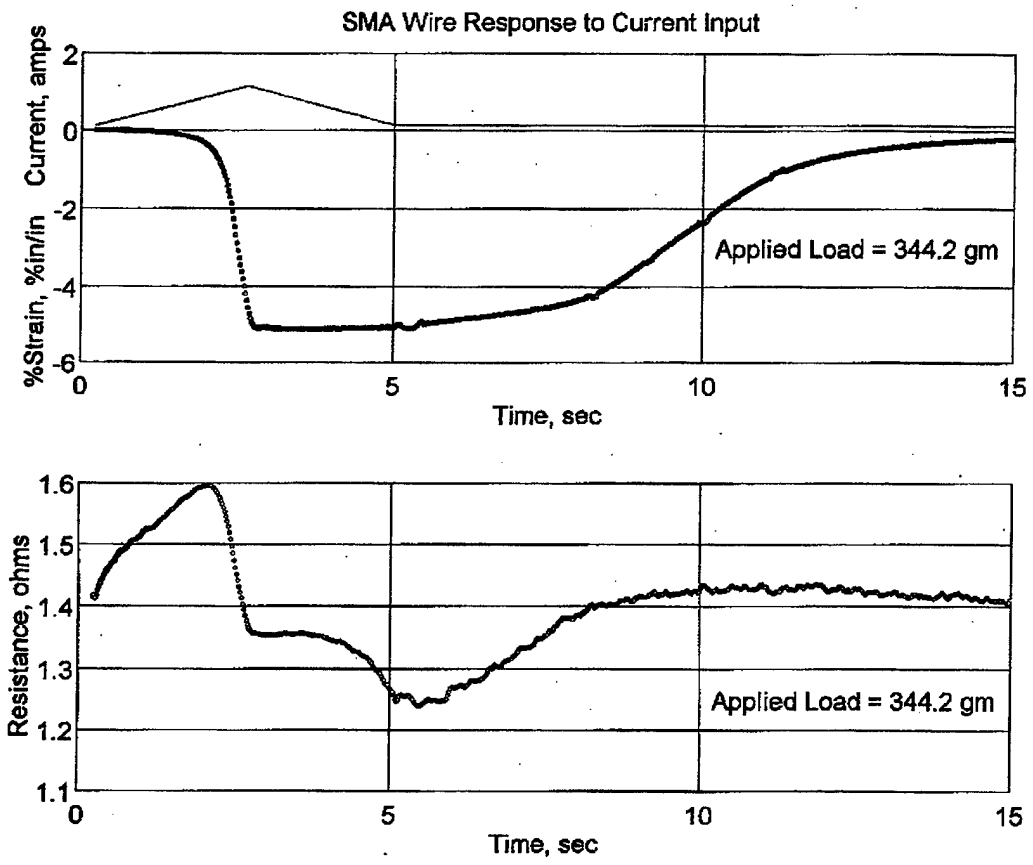

Figure 4.5 : Variable Load Test, 344.2 gm.

2. Constant Load Testing

For this series of tests, the load applied to the SMA test wire was maintained constant. The duration and magnitude of the electrical heating current was varied while the wire's resistance and strain were recorded. The function generator programming voltage signal shape was a step function and of sufficient magnitude such that the initial electric heating current was 1.0 amp, the maximum recommended continuous heating current. The duration of the step function was started at 5 seconds and reduced to the point that complete transformation did not occur. From this point, the amplitude of the current step function was increased while the time of the step duration remained constant. The parameters are summarized and listed in Table 4.3 for the constant load test of the SMA tests wire. Two plots, 1) current, resistance, and strain versus time and 2) resistance versus time, were generated for each data run using MATLAB® and are shown in Figures 4.6 through 4.13.

As the heating cycle time is reduced, a point is reached when the energy needed to cause a phase transformation is not meet. By increasing the magnitude of the electric heating current, the energy required is again reached and phase transformation occurs. From the evaluation of the heat transfer model in Chapter III, for a heating current of 2.0 amps, the heating time required to cause transformation was 8.4 times shorter than the time required to decay to the phase transformation point. Figure 4.12 is a plot of the 2.0 amp electric heating current and the SMA test wire's response. The heating cycle time was 0.5 seconds while the decay time was 2.5 seconds. The decay time measured is 5 times longer than the heating cycle time. The difference can be attributed the inaccuracies associated in simplification of the heat transfer model. It is important to note that the concept of thermal inertia introduced in Chapter III has been sufficiently demonstrated with this constant load testing.

In Figure 4.6 and 4.7, the resistance curve indicates that excess heating beyond what is needed to cause the phase transformation of the SMA wire is taking place. The

resistance of the SMA increases as the temperature of the wire increases. A sudden reduction in resistance occurs when the temperature of the wire passes through the austenitic start and then finish temperature points. As additional energy is supplied to the wire, the temperature continues to increases, resulting in an increase in the resistance of the wire. When the heating on the wire is stopped, the temperature of the wire starts to drop and the resistance also starts to decrease. At the martensitic start temperature, the resistance begins to increase as the transformation takes place. The increase in resistance continues to completion of the martensite transformation and then the resistance begins a gradual reduction due to cooling of the wire.

Constant Load Testing

constant load : 237.2 gm				wire length (austenite) : 8.13 cm		
				ambient temperature : 23.0 °C		
Heating current	heating cycle time	% strain	Ω, austenite	Ω, martensite	% Ω change	transformation time
1.0 amp	5.0 sec	-4.73	1.18	1.36	13.24	6.0 sec
1.0 amp	2.5 sec	-4.62	1.2	1.38	13.04	3.0 sec
1.0 amp	1.5 sec	-4.53	1.21	1.39	12.95	1.0 sec
1.0 amp	1.0 sec	-3.85	1.25	1.39	10.07	0.5 sec
1.0 amp	0.5 sec	-0.51	1.41	1.36	-3.68	-0 sec
1.5 amp	0.5 sec	-4.43	1.22	1.38	11.59	0 sec
2.0 amp	0.5 sec	-4.63	1.21	1.39	12.95	2.5 sec
2.5 amp	0.5 sec	-4.57	1.2	1.37	12.41	3.0 sec

Table 4.3 : Constant Weight Test. Test parameters and results for the constant weight testing of the SMA test wire.

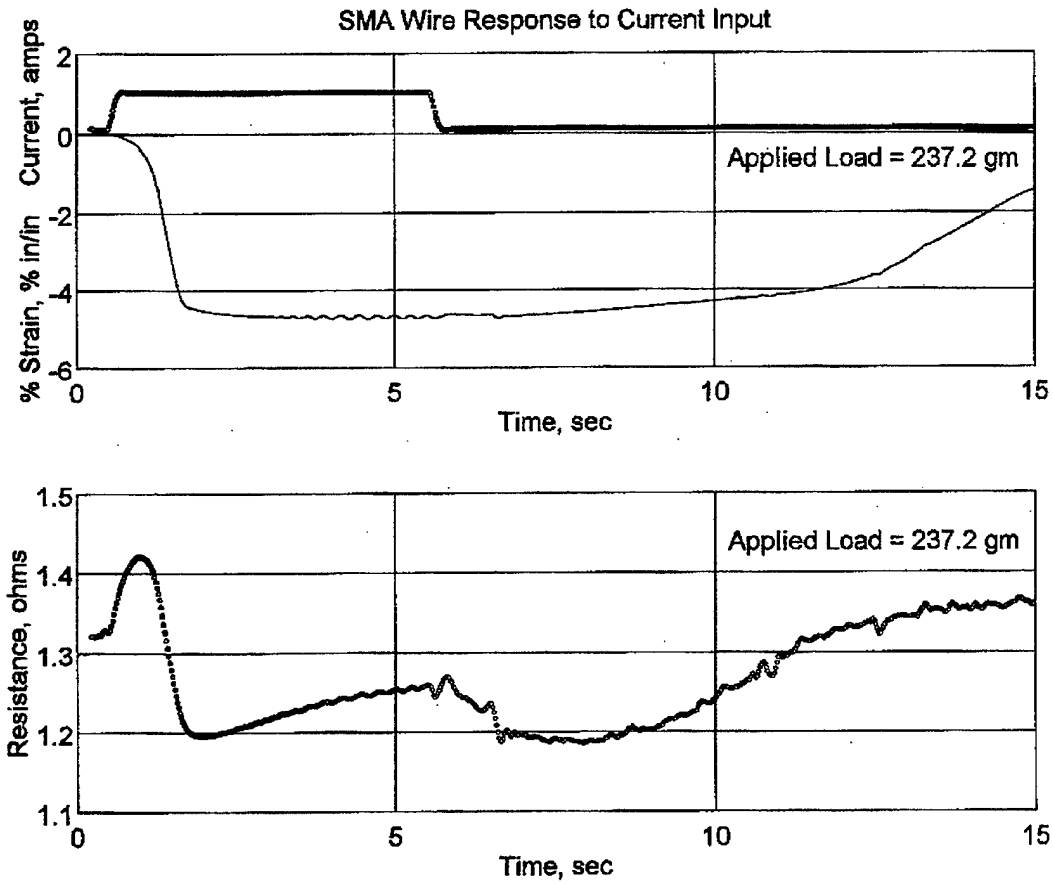

Figure 4.6 : Constant Load Test, th = 5.0 sec, Is = 1.0 amp.

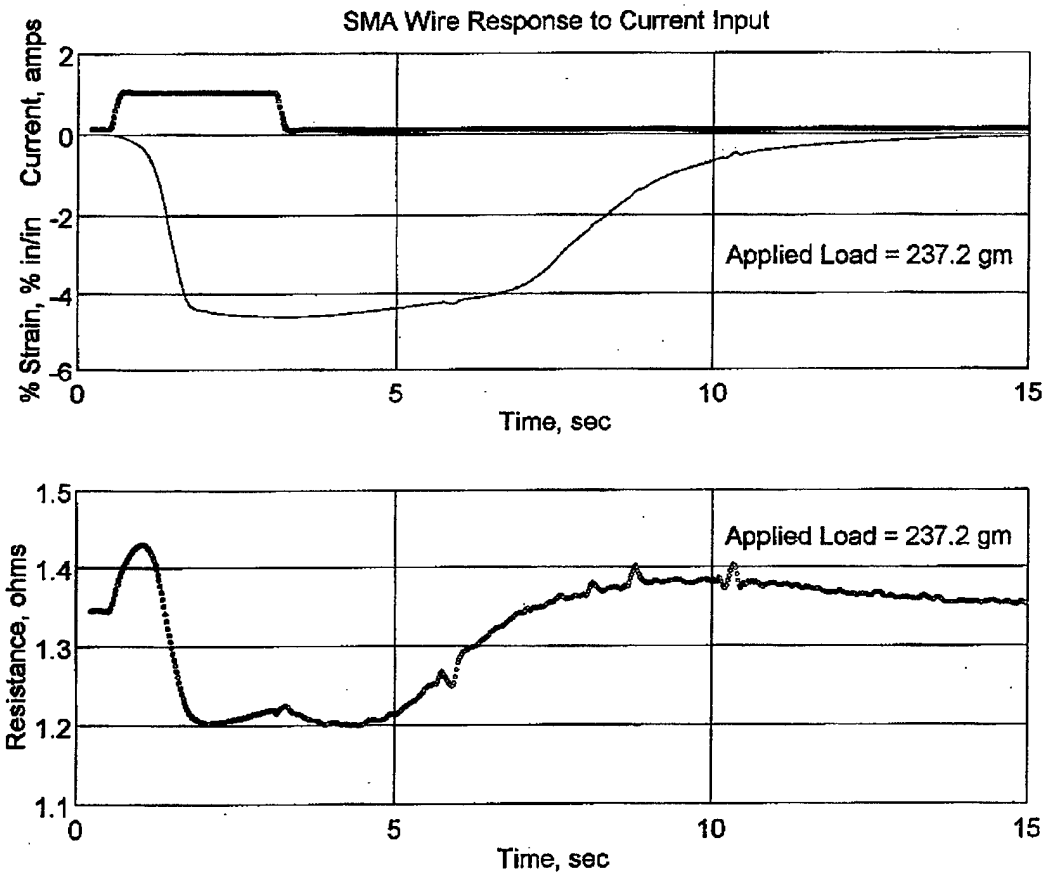

Figure 4.7 : Constant Load Test, th = 2.5 sec., Is = 1.0 amp.

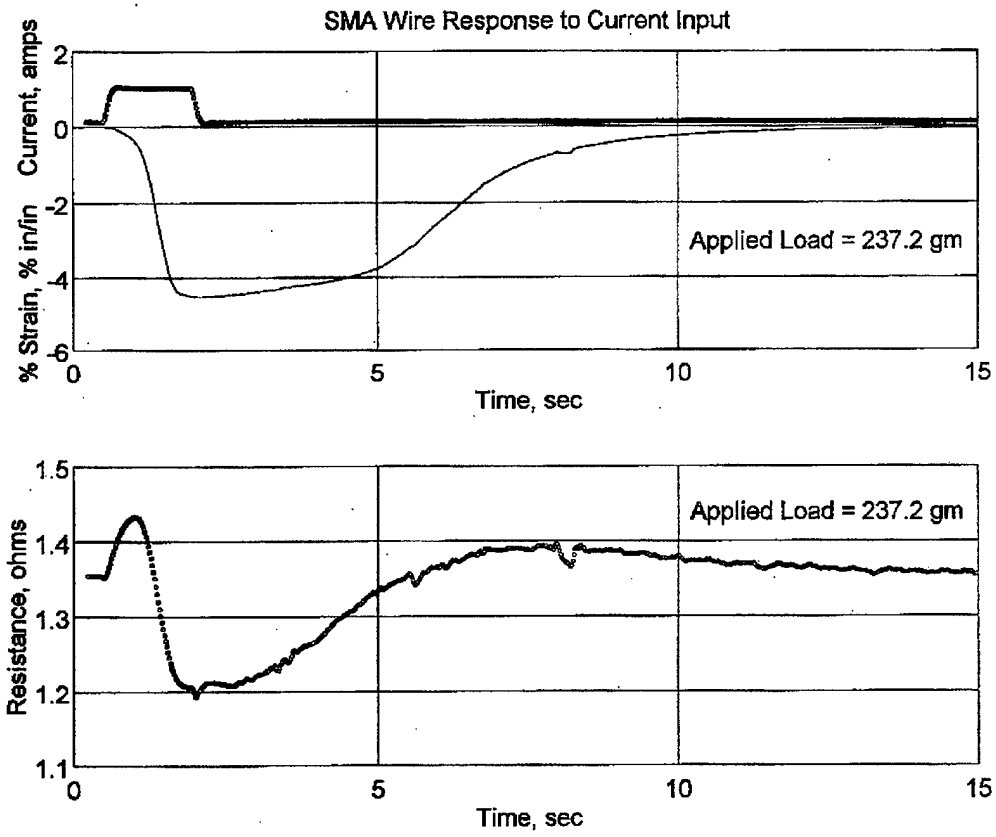

Figure 4.8 : Constant Load Test, th = 1.5 sec., Is = 1.0 amp.

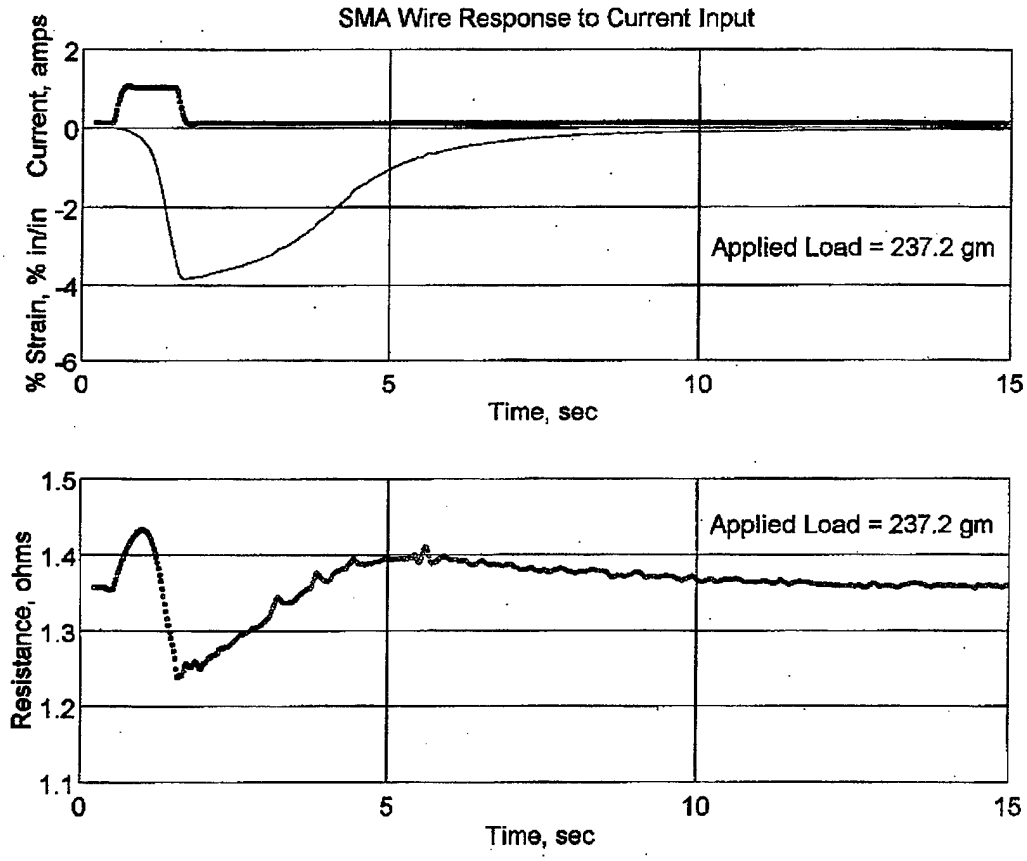

Figure 4.9 : Constant Load Test, th = 1.0 sec., Is = 1.0 amp.

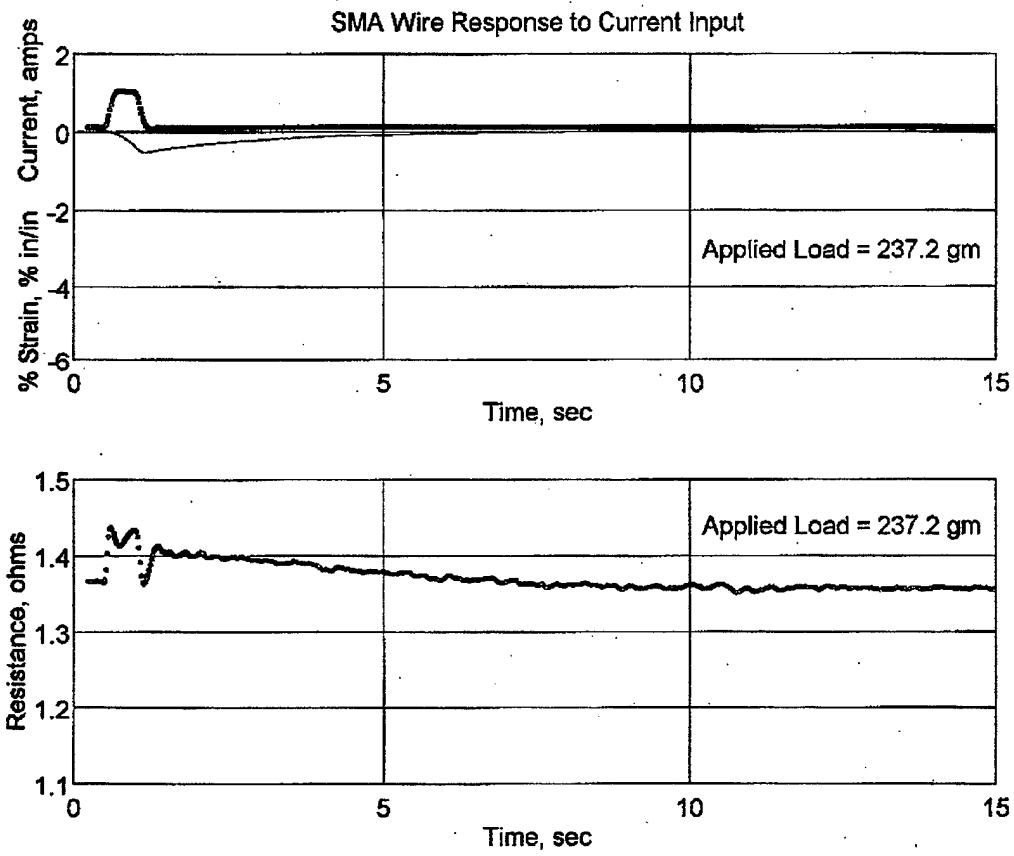

Figure 4.10 : Constant Load Test, th = 0.5 sec., Is = 1.0 amp.

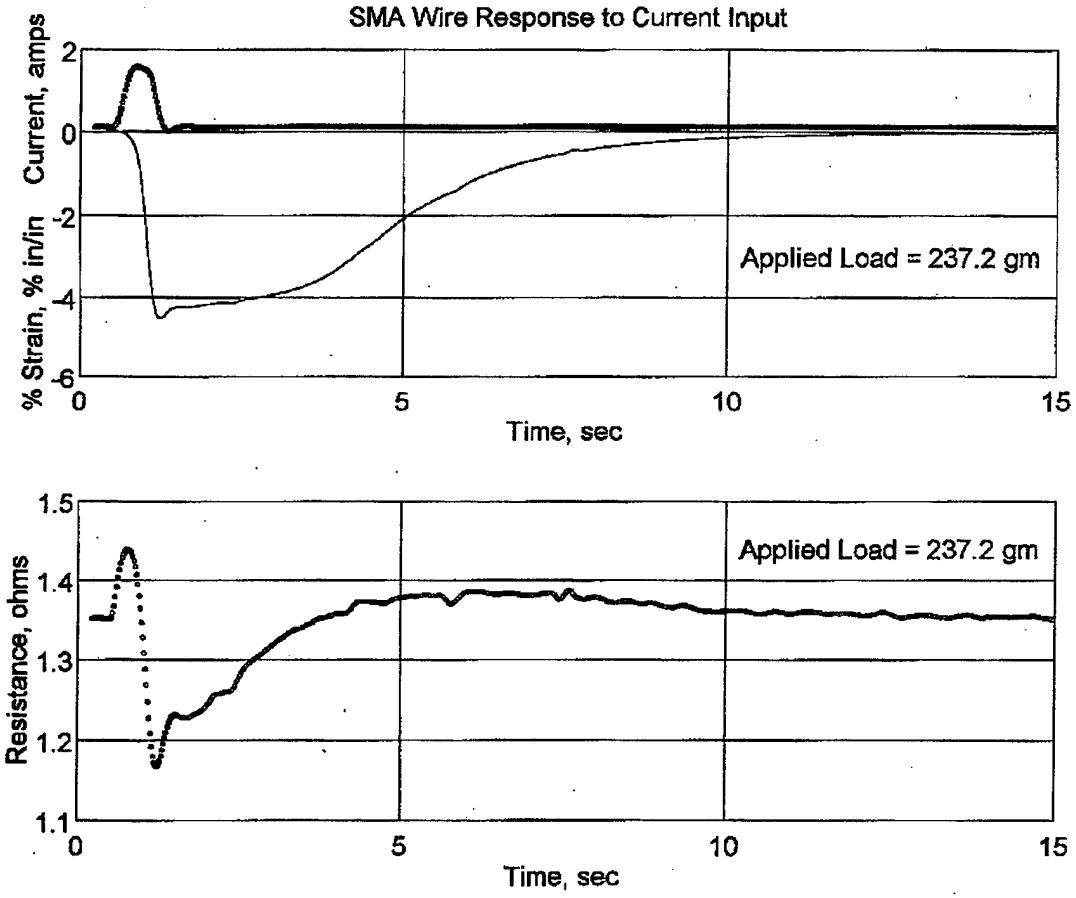

Figure 4.11 : Constant Load Test, th = 0.5 sec., Is = 1.5 amp.

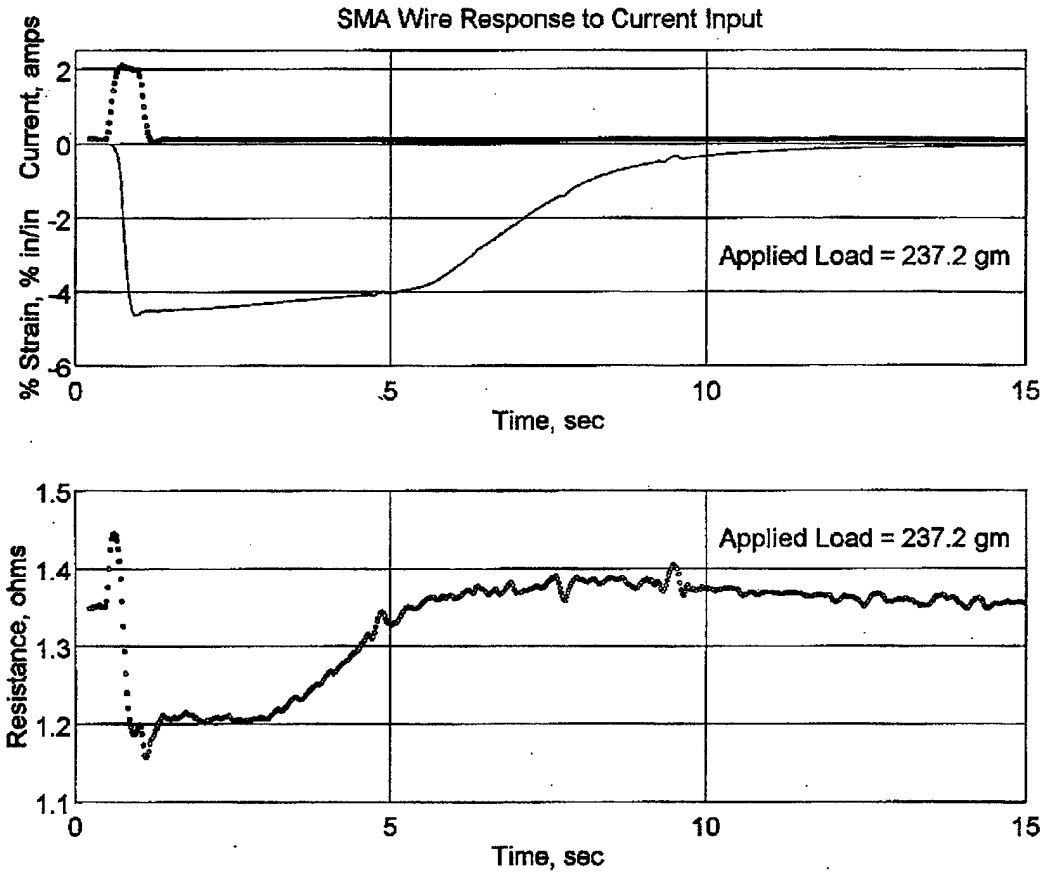

Figure 4.12 : Constant Load Test, th = 0.5 sec., Is = 2.0 amp.

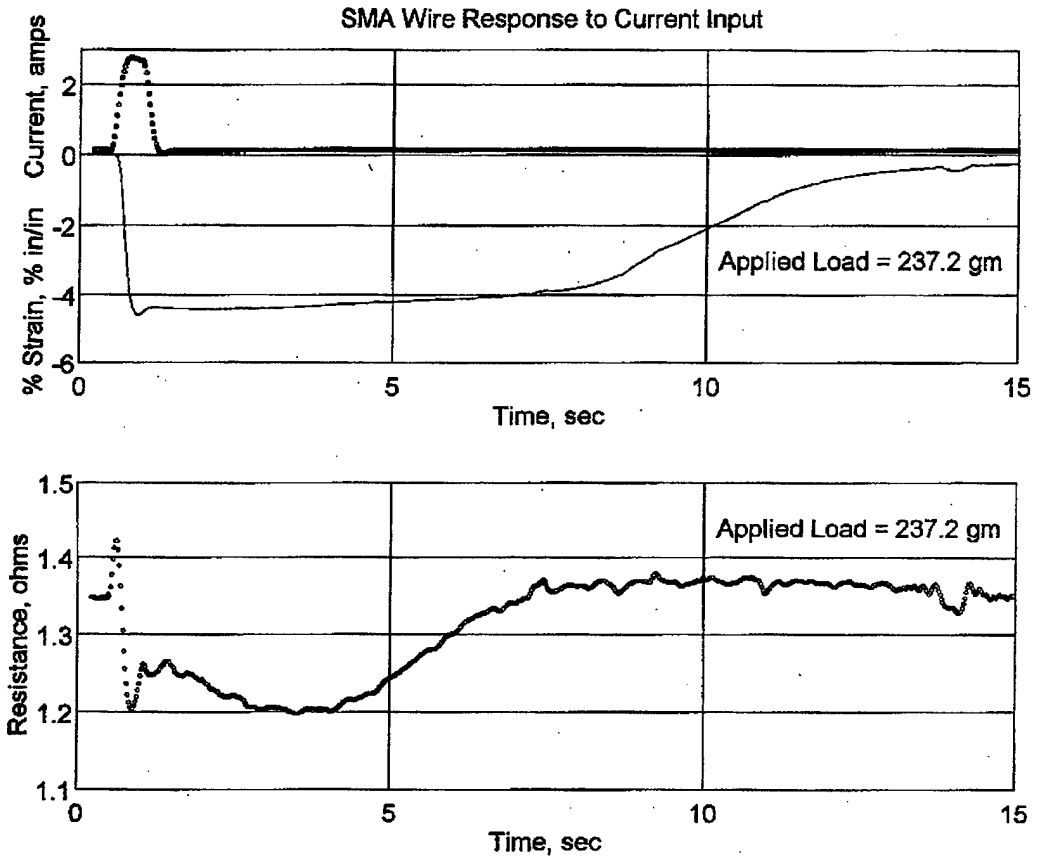

Figure 4.13 : Constant Load Test, th = 0.5 sec., Is = 2.5 amp.

V. PROTOTYPE TEST BOARD AND ACTUATOR MATRIX DRIVER

In Chapter III, the notion of thermal inertia was introduced and was subsequently demonstrated in Chapter IV. Now a control and powering system for discontinuously heating the SMA elements of a manipulator is considered. This system will heat the SMA elements sequentially using a cycle of short current pulses and relatively long periods of no current. Due to thermal inertia, a SMA element can be alternately heated to phase transformation with a short current pulse and then no current applied while other elements are heated with a short current pulse. Before the SMA element can cool to the point of phase transformation, it is heated again by a short current pulse. This system is called the Actuator Matrix Driver (AMD) and is designed to use a minimum number of required leads by fully integrating the powering system with the control system.

The configuration of the SMA actuators was based on the physical dimensions and motion requirements of the manipulator. A prototype test board was designed to test the SMA actuator control and powering system and simulates the manipulator's intended design for SMA actuator location.

A. PROTOTYPE TEST BOARD

The size restrictions of the manipulator necessitated that the motion requirements be met with the minimum number of elements. Accordingly, 3D motion was realized through the use of three actuators per segment. For the initial investigation, the manipulator would be developed using a total of five (5) segments. The manipulator's actuator configuration results in a total of fifteen (15) SMA actuators. A test board was designed and constructed to simulate this arrangement.

1. Description

The SMA actuator prototype test board, designed and constructed to simulate the operation of the manipulator, is show in Figure 5.1. The prototype's base board is constructed of 0.5 inch Plexiglas with overall dimensions of approximately 12 inches wide by 25.5 inches long. Stiffening is provided by four 1 inch square ribs running lengthwise on the bottom side of the board.

Arranged on the base board are fifteen (15) SMA test elements in a 3 x 5 pattern. This pattern simulates the envisioned arrangement of SMA actuators intended for the manipulator design. The SMA test elements mimic an SMA actuator and its purpose is to indicate when a command has been successfully directed to and received by a SMA actuator. Each test element consists of two brass bolts anchored in the Plexiglas approximately eight (8) inches apart, a spring providing a bias return force, and a SMA wire. Indication is provided by an infra-red switch and a LED light. See Figures 5.2 and 5.3 for detailed drawings of an individual SMA test element. Successful receipt of a

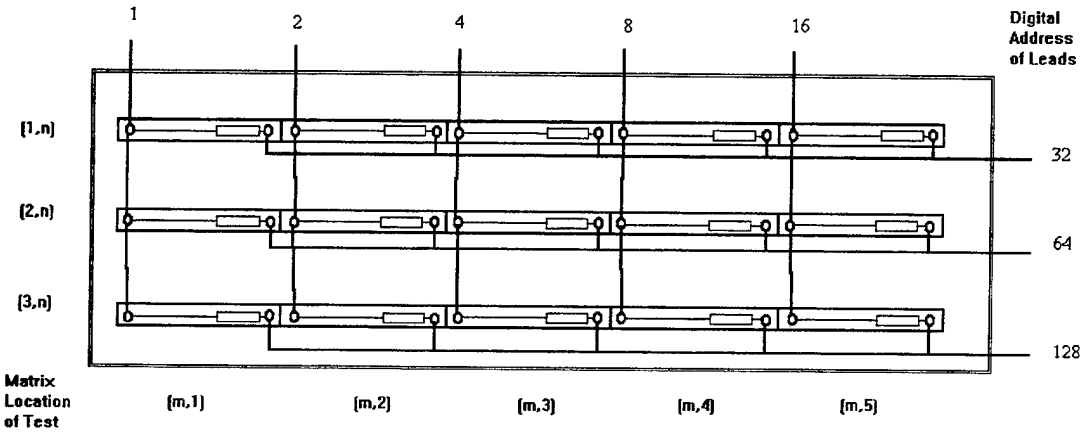

Figure 5.1: SMA actuator prototype test board. Show are the matrix location of the SMA test elements and the digital number assignment of the lead used for control and power of the test elements.

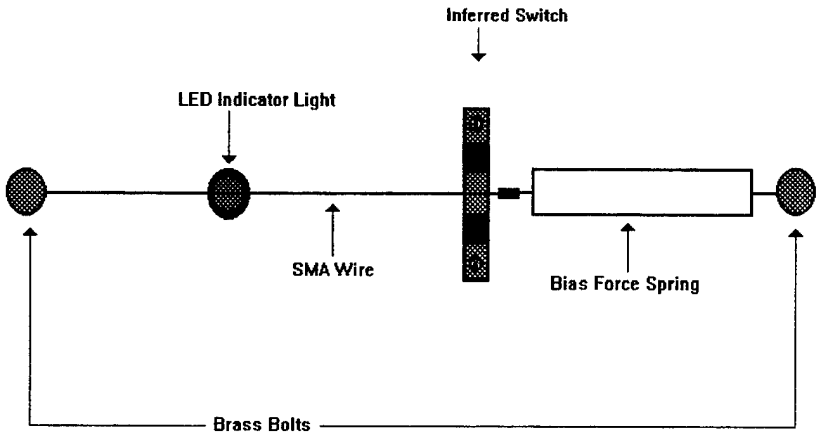

Figure 5.2: SMA test element, top view. Each test element is composed of two brass bolts anchored into the test board, LED indicator light, infra-red switch, bias force spring, and SMA wire.

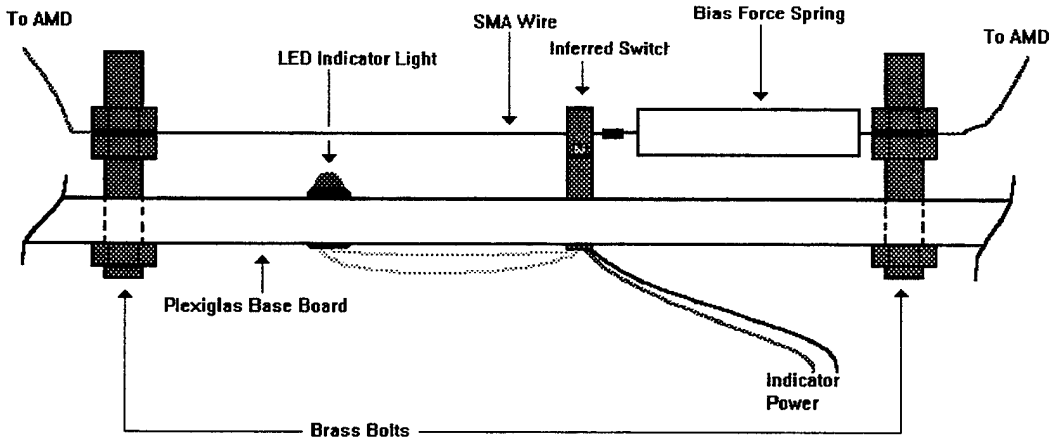

Figure 5.3: SMA test element, side view. The connector between the bias force spring and the SMA wire blocks the infra-red beam of the switch. This causes the LED indicator to light, indicating that the wire has contracted.

command signal results in the contraction of the SMA wire. This causes the infra-red beam of the infra-red switch to be block by the wire to spring connection. Interruption of the beam sends current to the indicator light which turns on to mark that the wire command has been properly sent, received, and executed. The test elements are connected in a matrix pattern as shown in Figure 5.1. One end of each SMA test element is connected together within each column and the opposite end of the SMA actuators are connected together within each row. The result is a total of eight leads as show in Figure 5.1.

2. Operational Numbering Scheme

A numbering scheme is assigned to the SMA test elements such that the columns of SMA test elements are number one through three and each row numbered one through five. Therefore, the upper left test element in Figure 4.1 is (1,1) and the lower right test element is (3,5). The test element (2,3) is located in the second column and is the third element from the left.

Each lead is assigned a digital address number in the base 2 system, i.e. 1, 2, 4, 8, 16, 32, 64, and 128. Refer to Figure 5.1 for the numbering sequence of the leads. The digital address system will be used to access the leads which control the SMA test elements. Therefore, to access SMA test element (2,4) , leads numbered 8 and 64 must be selected. For access to SMA test element (3,1), leads 1 and 128 must be selected.

From this matrix type arrangement, the number of leads needed to access the SMA test elements is significantly reduced from what would normally be expected. If a conventional means of actuation and control were used, each SMA test elements would have a minimum of two leads per element and the total number of leads would be 30. A common ground system could reduce the number of leads to 15 active leads and one ground lead for a total of 16 leads. By using this matrix connection, the number of required leads is reduced to only eight (8), a reduction of almost 50%. As the number of

segments is increased, the conventional method with a common ground of actuation adds three lead wires per segment and requires ($3n$+1) lead wires for n segments. The matrix connection adds a single lead wire for every additional segment and requires (n+3) lead wire for n segments.

B. ACTUATOR MATRIX DRIVER BOARD

The use of only eight leads for access to the SMA test elements requires a system that is able to directly power to the matrix of test elements and use the same leads for measuring the electrical condition of each element. A system was developed to facilitate these desired actions and is called the Actuator Matrix Driver. The Actuator Matrix Driver (AMD) sends power to the intended SMA test element while simultaneously providing for the monitoring of the electrical condition of that test element.

1. Description

The AMD consists of three external interface units and a control board which determines the magnitude of power sent to the test elements and which elements receive power. The three external interface units allow for control from a computer system to be received by the AMD, for the monitoring of the test elements by the computer system, and for the connection of the test element leads and power source to the AMD. The two external interface units used to transfer data between the AMD and the computer are 50 pin connectors. These two 50 pin connectors make up to a 100 pin cable compatible with a personal computer installed data acquisition board. The final external interface unit is a 24 port wire connector. It has the capability of providing twelve simple point to point connections. Figure 5.4 is a diagram showing the AMD's overall physical layout and component location.

The AMD control board is composed of a 74LS240 inverting buffer, three PNP column driver transistors, five NPN row driver transistors, and one NPN power amplifier transistor. A LM7805C 5 volt regulator and miscellaneous driver transistors, diodes and resistors complete the component list. Figure 5.5 is a schematic diagram of the AMD's interface units and the wiring scheme of the SMA test elements. Figure 5.6 is a schematic diagram of the AMD control board showing the components and pin connections of the board. Refer to Figures 5.5 and 5.6 for component and pin location.

The actuator matrix driver is composed of three identical current amplifiers which have a common input control voltage. Each current amplifier is in series with a solid-state

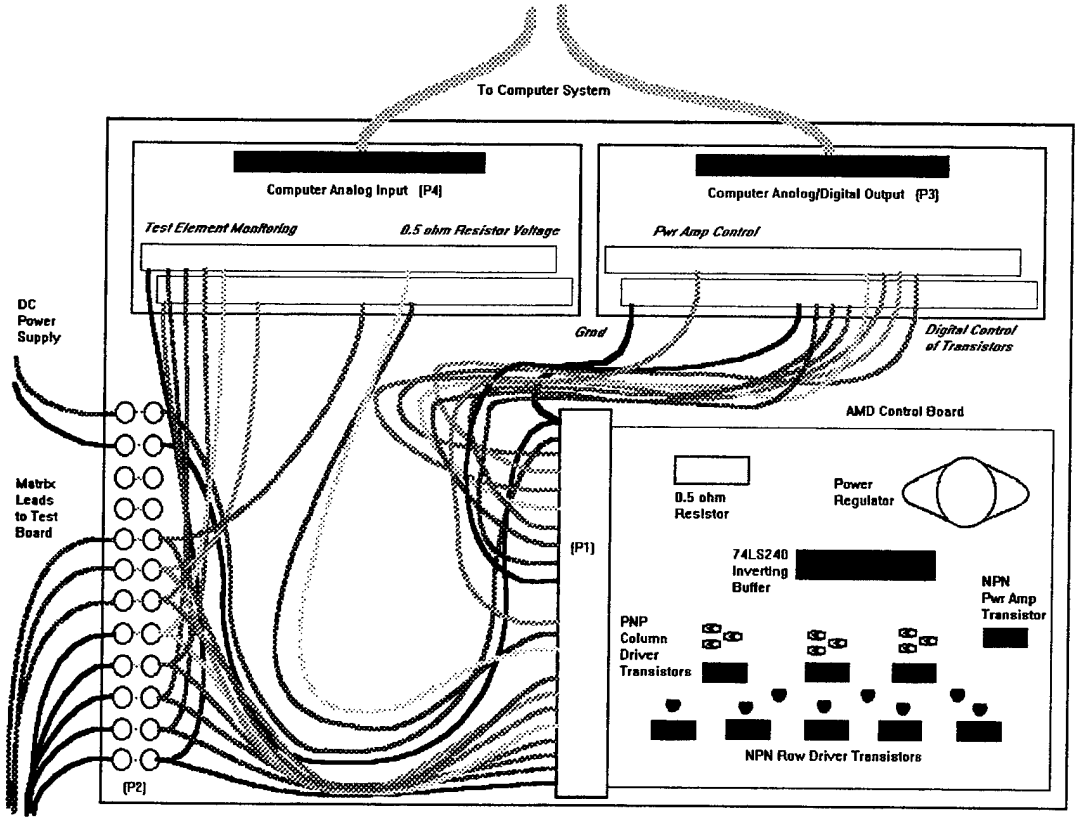

Figure 5.4: Diagram of the Actuator Matrix Driver (AMD). Diagram shows the overall physical layout and component location of the AMD.

switch. These switches, R1, R2 and R3, form the 'column' drivers of the matrix. Five additional solid-state switches, R4 through R8, form the 'row' drivers of the matrix.

Bits 0 through 4 of the computer digital output are connected via connector P2 pins 7 through I to the driver networks for the row-drive solid-state switches. The row outputs are on PI pins I through 5. Bits 5 through 7 of the computer digital output are connected via connector P2 pins 4 through 6 to the driver networks for the column-drive solid-state switches. The column outputs are on connector PI pins 6 through 8.

A regulated 12 V, 250 Watt, switching DC. power supply (VCC source and VEE) feeds the current-amplifier power transistors. Each current amplifier is composed of two MJ0030 power transistors, a 0.09437 Ω precision resistor, an MC3358 dual amplifier, and various resistors, diodes and capacitors. VDD for the MC3358 operational amplifiers is provided by VCC and an additional 5 V bias power supply. The output current (VSS) through the precision 0.09437 Ω resistor is sampled by the amplifier and used to control the absolute value of the current. The computer dialital-to-analog converter output is connected to the current-amplifier inputs via P1C pin 8. Three identical high-speed precision current amplifiers are used for redundancy. Each is individually connected in series (as the VSS source) to one of the three column' solid-state switches.

The resistance is measured from the value of the current pulsed through the individual SMA elements and the voltage drop across these elements. In order to measure the voltage across each SMA element, the computer's analog-to-digital multiplexed channel inputs at P1A and P1B are connected via JI through a modified DT-709Y to the matrix. The DT-709Y differentially samples the voltages across the SMA elements, amplifies them, provides an offset proportional to the current pulse and delivers a single-ended voltage to the analog-to-digital converter's multiplexed inputs. The amplification and offset are required to provide a higher degree of resolution for the voltage measurement.

Three sets of five of the DT-709Y input channel's 'Hi' inputs are wired in parallel to TB2 pins 2 through 16. Five sets of the DT-709Y input channel's 'Lo' inputs are wired

in parallel to TB I pins 2 through 16. This arrangement is connected to the eight wire drive lines on PI pins I through 8 and allows the voltage on each wire to be individually sampled. The computer digital-to-analog command voltage is also routed to the DT-709Y offset control line at W17/18 (not shown in the diagram). This allows the measured; voltage to be amplified by a factor of 10 for increased resolution. D.C. power to the DT-709Y is fed via J1 pins 19 and 20 from P1A.

2. Operation

The 15 SMA elements are individually heated by using the pulsed short current which is sequentially routed through the SMA element matrix composed of three columns and five rows. Digital output from a computer determines which positive column driver transistor is closed. This allows power from the unregulated DC power supply to be sent to the selected column of SMA test elements. The power sent to the SMA test elements is regulated by the AMD control board power amplifier. The power amplifier is controlled by an analog voltage signal from the computer. The circuit is completed by closing a selected row transistor via digital output from a computer. This connects a row of SMA elements to ground. A tightly controlled and highly accurate current pulse is now applied to the SMA element which results from the selected column and row transistor combination. Monitoring of the power applied to the selected SMA element is through a separate parallel connection point on the AMD. The voltage drop across the selected SMA element is sampled and used with the value of the pulsed current to determine its resistance via Ohm's Law. The computer is programmed to generate duty cycle pulse for each SMA element, the duration of the duty cycle being dependent on number of SMA Elements to be actuated. The amplitude of the current pulse is adjusted to ensure the SMA elements is heated to the required level needed for phase transformation. For the manipulator considered, a maximum of 10 elements, two per segment, may be actuated at any given time.

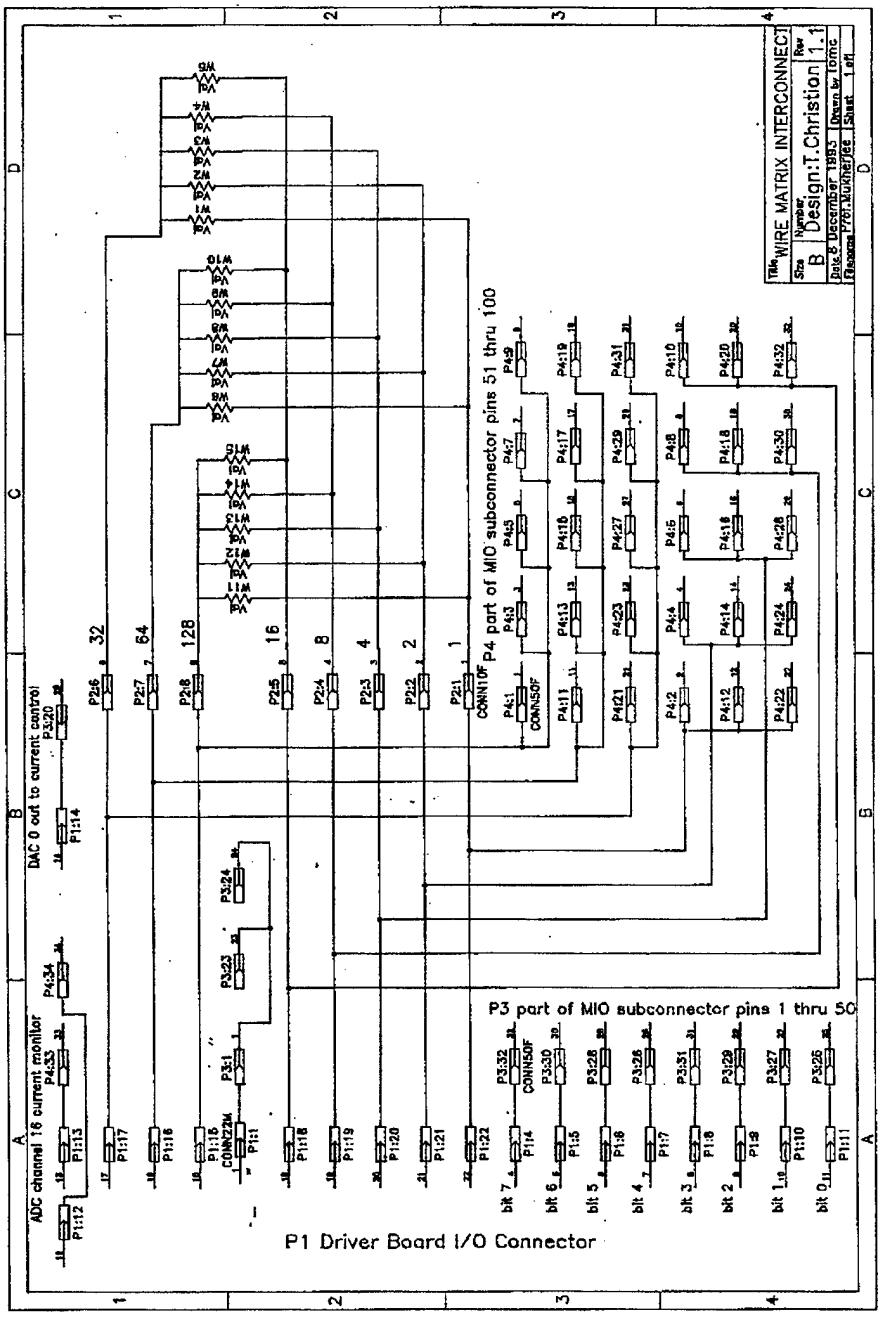

Figure 5.5 : Schematic diagram of the AMD's interface units and the wiring scheme of the SMA test elements.

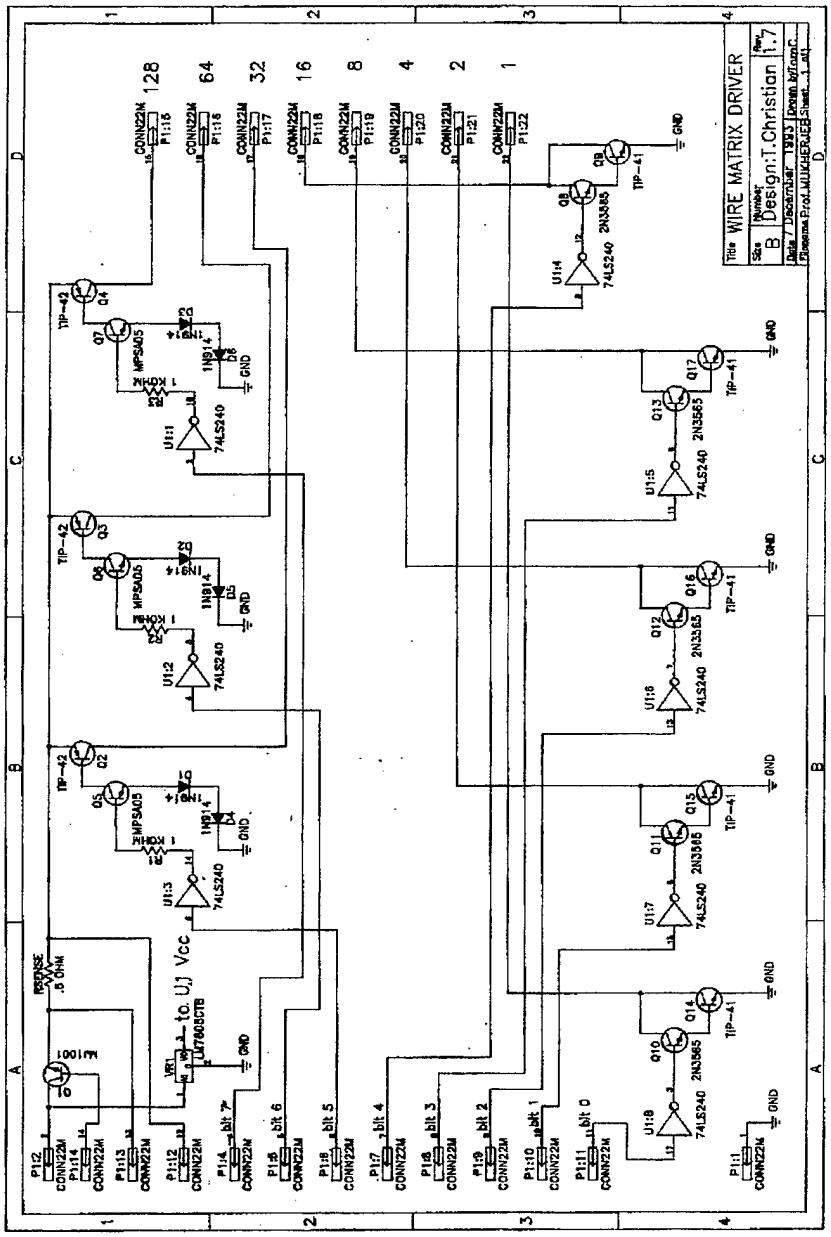

Figure 5.6 : Schematic diagram of the AMD control board showing the components and pin connections of the board.

VI. SMA ACTUATOR CONTROL SYSTEM

A scheme for powering the SMA test elements was developed based on the SMA's behavior that was observed in the resistance and strain response to current testing. The AMD directs power to the matrix of SMA actuators and allows for the simultaneous monitoring of these actuators. To control the AMD, a computer software program was developed for use on a DOS based Personal Computer (PC) which utilizes a Data Acquisition board to facilitate the performance of commands and the collection of data. Figure 6.1 is an overall diagram of the SMA actuator control system.

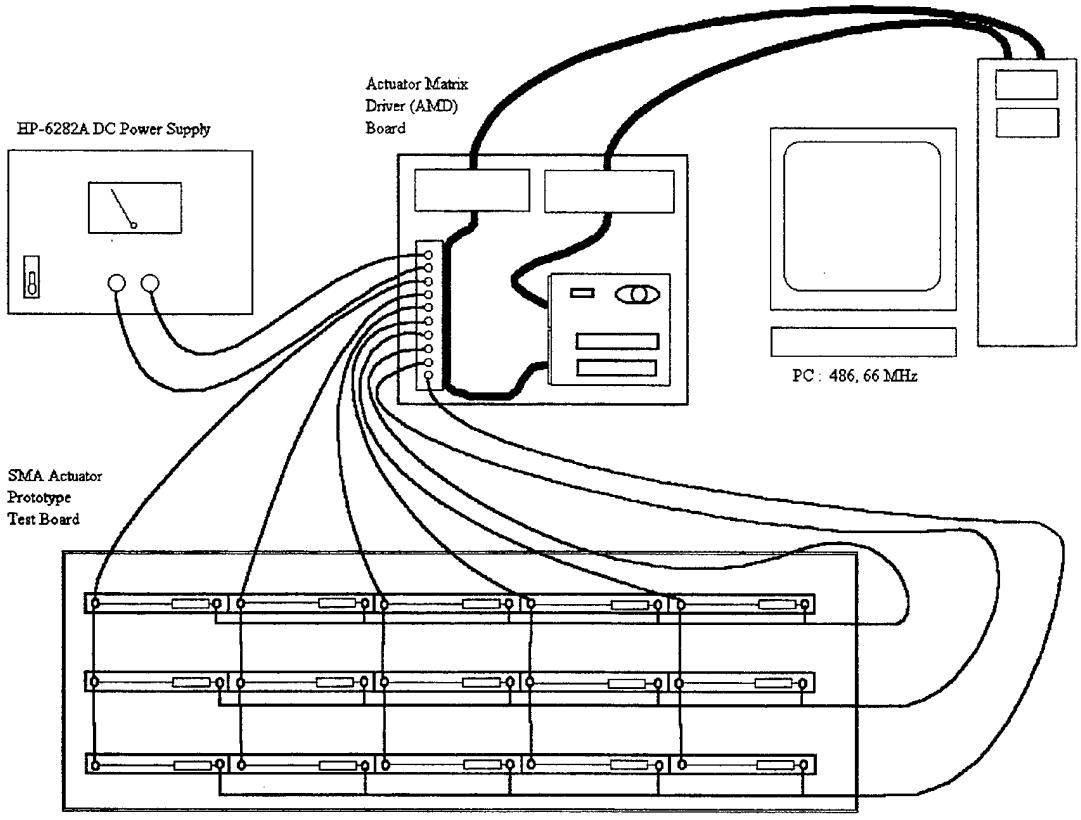

Figure 6.1 : SMA Actuator Control System. All major components are shown which comprise the system prototype for testing.

The 15 SMA elements are individually controlled and monitored using the matrix connection composed of three columns and five rows. The computer digitally selects a row and column and generates tightly controlled and highly accurate current pulse. The AMD, via an analog-to-digital converter with a multiplexed channel input, is used to sample the voltage drop across each SMA element. Using the values of the current pulse and the sampled voltage, the resistance of the SMA elements can be calculated using Ohm's law. The computer is programmed to generate a pulsed current with a specified duty cycle for each SMA element. The pulse amplitude is adjusted to allow the wire to heat to the proper level.

A. CONTROL SYSTEM HARDWARE

1. Personal Computer (PC) System

Control of the manipulator is performed by an IBM compatible personal computer (PC) with an analog and digital I/O data acquisition board installed. The PC system consists of a 80486-66MHz DX2 ISA mother board including an Intel 80486 processor with an integrated enhanced numeric coprocessor, 32-bit local bus, 16 MB of RAM, and a 540 MB hard disk.

2. Data Acquisition Board

The data acquisition board is a National Instruments® AT-MIO-64F-5 multifunction I/O board which features: 12-bit ADC, 200 kHz sampling rate, up to 64 analog inputs, 8 digital I/O , and two 12-bit DACs with voltage outputs.

B. COMPUTER SOFTWARE PROGRAM

The computer program was developed using the LabVIEW® application software package. LabVIEW® is a graphical icon based software programming system for instrumentation. Programs are written using LabVIEW® by graphically assembling software modules or virtual instruments (VIs), represented by program icons, into an executable program. The LabVIEW® program "Wire Control & Status.vi" is enclosed in Appendix C.

The program has two parts, the Front Panel and the Block Diagram. The front panel is where the operator controls which elements of the manipulator are to be energized. The operator can also control the duty cycle by slowing down the loop sequence of the program and can also control the amplitude of the pulsed current sent to each group of wires. There is also status graphs to see how the elements are operating. The block diagram is the actual program. It provides a visual representation of the data flow as it would actually occur. Programming is accomplished in LabVIEW® by selecting the functional type icons to be used in the program and wiring them up into a working block diagram that direct the flow of data.

For control of the manipulator, the front panel is used. A double set of three Wire Control Boards is used to control the manipulator. The upper set is the command group. A mouse is used to highlight the numbered light that corresponds to the actuator element to be energized. The lower set of boards returns a lighted signal when the actuator element is energized. The amplitude of the pulsed current sent to each group is controlled individually with the slide gages below the control boards. Three real time graphs monitor the resistance of each SMA wire test element within each group. These graphs are located on the front panel below the controls mentioned above.

The block diagram listed in the Appendix B displays only the loop for the first group of actuators, but the loops are identical for all three groups. The outer large block is a while loop and continues to operate the program inside as long as there are no errors

and the stop button is not engaged. The icons to the left of the while loop are concerned with configuring the computer system and data acquisition board. It should be mentioned that each icon is a subprogram all its own. These icon subprograms may be simple routines or may be very complex program in their own right, depending on the purpose of the icon. Double clicking on a icon brings up to the screen of the particular subprogram. Each level in turn has a series of icons which contain a set of programming all there own which in turn contain more icons, etc. Only the top level will be discussed.

Contained within the while loop are the logical stop controls, the loop delay for minor time control, and a sequence frame. The sequence frame controls the sequential progression of the program from one group or column of actuators to the next and then starts over again. Inside the sequence frame is a for loop which executes the same number of times that there are actuators in each group. Within the for loop is located the Boolean controls which get their commands from the front panel wire control boards. Based on the light combinations on the front panel, a number is generated for use in digital addressing. The program then sequentially steps through the routine, determining if a SMA actuator gets power at the level specified on the front panel.

Simultaneously, the same address information is going to the monitoring section within the for loop. The voltage drop across a SMA wire is measured, then the voltage drop across a precisely calibrated resistor on the AMD board is used to determine the actual current through the wire. Using Ohm's Law, the resistance is calculated for the SMA wire. This data is sent to the front panel for display and monitoring.

When an error is received or the stop button is engaged, all operations are halted and the block to the right of the loop takes over. Its purpose is to return all port openings to a safe condition so than no miscellaneous power is circulating through the system.

C. EXPERIMENTAL RESULTS

Experiments were conducted with the SMA Actuator System described above. The SMA elements were controlled in open-loop mode because the primary objective was to use the AMD to demonstrate that multiple SMA elements could be actuated using fewer lead wires. The performance of the open-loop control was judged from the resistance plots. The computer program via AMD has provisions for measuring the resistance of the SMA elements, therefore closed-loop control of the SMA elements using resistance feedback can be incorporated by simply modifying the software for the control of the SMA elements.

It was discussed earlier that among the 15 SMA elements, a maximum of 10 elements would be actuated simultaneously at any given time. Therefore, the program operated any combination of up to 10 SMA elements, maximum of two per segment. For the maximum number of SMA elements actuated, the current pulse operated on a *10%* duty cycle. The experimental results for a single SMA element are shown in Figure 6.2. Figure 6.2 shows the variation in the resistance of the SMA wire as the wire is actuated by a current pulse of 1.6 A, 6 ms in duration and a 10% duty cycle. The wire had an initial resistance of 2.1 Ω and the total resistance in the lead wires was approximately 0.6 Ω. Figure 6.2 shows that the resistance drops almost immediately from 2.7 Ω to around 2.5 Ω. Previous experiments have shown that the austenitic resistance of an SMA is approximately 10% less than the martensitic resistance. Therefore, Figure 6.2 indicates that the pulse current is able to maintain the wire in its austenite state at all times. The results in Figure 6.2 indicates that the AMD can be used effectively for the control of multiple SMA elements using fewer lead wires.

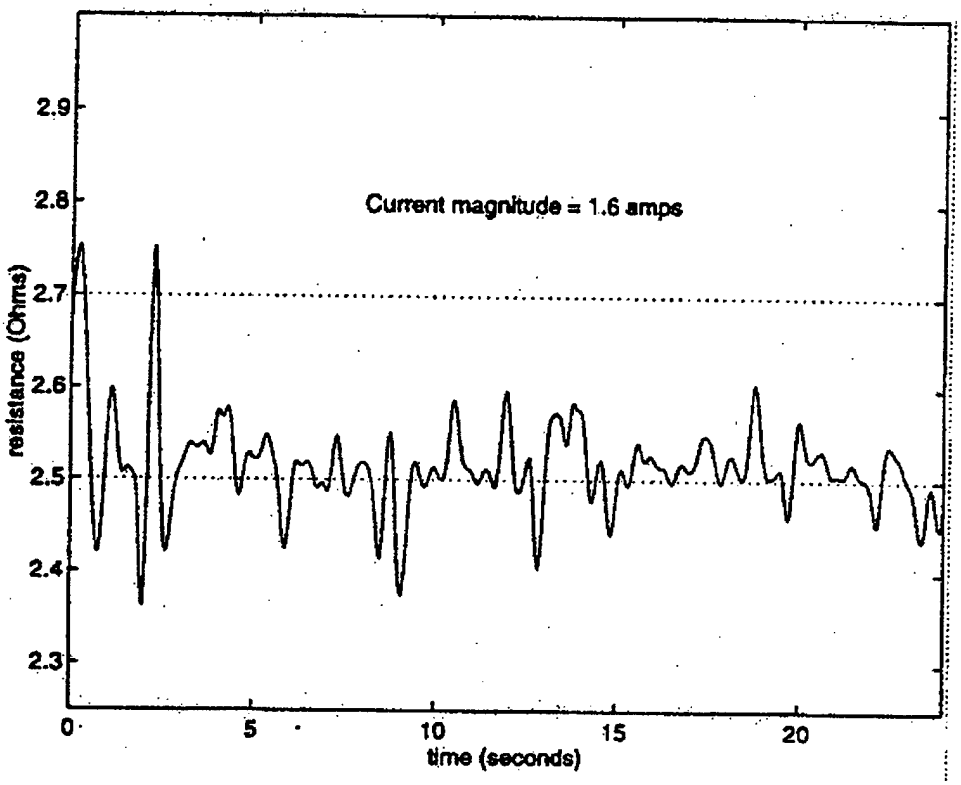

Figure 6.2 : Variation in the resistance of a SMA wire with time for the case where the current pulse duration was 6 ms and the duty cycle was 10%.

VII. RECOMMENDATIONS AND CONCLUSIONS

A. RECOMMENDATIONS

SMA material return to it austenitic shape when heated to its phase transformation temperature. Upon cooling, it forms martensite. The amount of elongation the material undergoes is dependent on the stress applied. Therefore, if the material was used to effect a motion upon contraction, the return to its normal position would be dependent on the internal bias force plus the external load. With only resistance to determine status of the actuation elements, the exact position would be unknown. A two way shape memory material with a more defined motion or a superelasticity material also with defined motion that does not rely on an external force for its motion.

LabVIEW® can be a very versatile programming tool. It provides not only data control and processing but a visual aid for control and processing. This visual aid in computer programming has a cost in speed. Screen updates significantly slow down the system's ability to process data. Also, LabVIEW® operating system clock uses the internal PC clock which is not very dependable and subject to management problems with software and hardware interrupts. It is recommended that a faster system be used with a more reliable time system.

B. CONCLUSIONS

This thesis presents a digital control system used for the control of a manipulator composed of SMA actuators or elements. SMA exhibits very defined physical property changes and behavior as the temperature is varied and the material undergoes phase transformation. The behavior of SMA was estimated by evaluating a heat transfer model of the SMA element. This heat transfer analysis provided an expected behavior for the SMA element and lead to the introduction of the concept of thermal inertia. Thermal

inertia allows for SMA elements arranged in a matrix form to be individually heated by a tightly controlled and highly accurate short pulsed current followed by a significant off time. During the off time, other SMA elements are sequentially heated. Resistance monitoring is acceptable for determining the phase of the material. Resistance is not adequate for determining the amount of strain recovered or given up. Therefore, position determination with only resistance information is inappropriate. The principle of discontinuous heating with sequential powering, control, and monitoring allows the number of leads to be reduced by 50 percent, just eight leads for a system with 15 SMA elements. The actuator matrix driver (AMD) was developed to control and monitor the matrix of SMA elements. The results of monitoring a single SMA element indicates that the open-loop mode actuation system effectively controlled the matrix of 15 SMA elements. Closed-loop control of the matrix of SMA element can be accomplished by modifying the computer software program.

APPENDIX A. HEAT TRANSFER MODEL CALCULATIONS

Appendix A : Heat Transfer Model Calculations

SMA Wire Characteristics*

Density : $\rho := 0.235 \cdot \frac{lb}{in^3}$ $\rho = 6.505 \cdot \frac{gm}{cm^3}$

Specific Heat : $C_p := 0.20 \cdot \frac{BTU}{lb \cdot R}$ $C_p = 0.2 \cdot \frac{cal}{gm \cdot K}$

Heat of Transformation : $h_t := 10.4 \cdot \frac{BTU}{lb}$ $h_t = 24.19 \cdot \frac{kJ}{kg}$

Thermal Conductivity : $k := 10.4 \cdot \frac{BTU}{hr \cdot ft \cdot R}$ $k = 18 \cdot \frac{watt}{m \cdot K}$

Linear Resistance :

nominal : $\Omega_m := 0.44 \cdot \frac{ohm}{in}$ $\Omega_m = 0.173 \cdot \frac{ohm}{cm}$

Electrical Resistivity :

Martinsite : $R_m := 421 \cdot \frac{ohm}{cirmil \cdot ft}$

Austinite : $R_a := 511 \cdot \frac{ohm}{cirmil \cdot ft}$

* - SMA wire characteristics provide by manufacturer of Flexinol™ Actuator Wires,
Dynallooy, Inc.
Makers of Dynamic Alloys
Irvine, CA 92715

Transformation Temperatures :
(as determined from Resistence - Temperature measurements)

$T_{As} := 343 \cdot K$ $T_{Af} := 363 \cdot K$

$T_{Ms} := 353 \cdot K$ $T_{Mf} := 331 \cdot K$

Appendix A : Heat Transfer Model Calculations (continued)

Test Wire Characteristics : Dimensions @ stated load :

load : $W := 237.2 \cdot gm$ % strain : $\%\varepsilon := 4.7$

diameter : $d := 0.01 \cdot in$ $d = 0.025 \cdot cm$

austenite : $La := 2.8285 \cdot in$ $La = 7.184 \cdot cm$

martensite : $Lm := La + \frac{\%\varepsilon}{100} \cdot La$ $Lm = 7.522 \cdot cm$

nominal length : $L := \frac{La + Lm}{2}$ $L = 7.353 \cdot cm$

volume : $V := \pi \cdot \frac{d^2}{4} \cdot L$ $V = 0.004 \cdot cm^3$

surface area : $A_s := \pi \cdot d \cdot L$ $A_s = 0.587 \cdot cm^2$

mass : $M := \rho \cdot \left(\pi \cdot \frac{d^2}{4} \cdot Lm \right)$ $M = 2.479 \cdot 10^{-5} \cdot kg$

Test Conditions :

monitor current : $I_m := 0.1 \cdot amp$

step current : $I_s := 2 \cdot amp$

ambient temperature : $T_{amb} := 296.2 \cdot K$

free convection
heat transfer coefficient : $h := 25 \cdot \frac{watt}{m^2 \cdot K}$

Test Sequence :

1) Initial monitoring with I_m current
2) Heating with step current, I_s
3) Cooling, post heat monitoring with I_m current

Appendix A : Heat Transfer Model Calculations (continued)

Test Sequence 1) - Initial monitoring with I_m current

rate of energy generation is equal to
rate of energy loss due to convetion: therfore, $ER_{st}=0$

$$ER_g=ER_{out}$$

$$I^2\cdot\Omega_m\cdot L=h\cdot A_s\cdot\left(T_i-T_\infty\right)$$

solving for the equilibrium temperature :

$$T_i:=\frac{I_m{}^2\cdot\Omega_m\cdot L}{h\cdot A_s}+T_{amb}$$

$$T_i=304.884\cdot K$$

Test Sequence 2) - Heating : neglect convective heat trasfer out of CV, $E_{out}=0.$

assume the energy input to CV is equal to the amount of energy required to heat wire to the transformation temperature plus the enegy required to cause phase transformation :

$$E_g=E_h+E_t$$

energy required to heat to transformation :

$$E_h:=\rho\cdot\left(\pi\cdot\frac{d^2}{4}\cdot Lm\right)\cdot C_p\cdot\left(T_{As}-T_i\right)$$

$$E_h=0.791\cdot joule$$

energy generation results in increase in energy storage(heating) : $E_g=I_s{}^2\cdot\Omega_m\cdot Lm\cdot\Delta t_h=E_h$

time to heat to transformation temperature :

$$\Delta t_h:=\frac{E_h}{I_s{}^2\cdot\Omega_m\cdot Lm}$$

$$\Delta t_h=0.152\cdot sec$$

Appendix A : Heat Transfer Model Calculations (continued)

energy of transformation : $E_t = M \cdot h_t$

during athermal phase transformation,
energy generated = energy of transformation : $E_g = E_h$

$$I_s^2 \cdot \Omega_m \cdot Lm \cdot \Delta t_t = M \cdot h_t$$

therefore, the time required to cause transformation :

$$\Delta t_t := \frac{M \cdot h_t}{I_s^2 \cdot \Omega_m \cdot Lm} \qquad \Delta t_t = 0.115 \cdot \text{sec}$$

Total time to transformation : $\Delta t := \Delta t_h + \Delta t_t$

$$\Delta t = 0.267 \cdot \text{sec}$$

Test Sequence 3) - Cooling, post heat monitoring with I_m current :

if assume no heat generation
(worst case situation) : $E_g = 0.$

loss of internal energy storage is
due to convective heat transfer : $-ER_{out} = ER_{st}$

use lumped capacitance method :

$$-\left[h \cdot (\pi \cdot d \cdot L) \cdot \left(T - T_\infty\right)\right] = \rho \cdot \left(\pi \cdot \frac{d^2}{4} \cdot L\right) \cdot C_p \cdot \frac{d}{dt} T$$

let : $\theta = T - T_{amb}$ then : $\frac{d}{dt}\theta = \frac{d}{dt} T$

energy balance equation becomes : $-(h \cdot (\pi \cdot d \cdot L) \cdot \theta) = \rho \cdot \left(\pi \cdot \frac{d^2}{4} \cdot L\right) \cdot C_p \cdot \frac{d}{dt}\theta$

simplifying : $$-\left(h \cdot A_s \cdot \theta\right) = \rho \cdot V \cdot C_p \cdot \frac{d}{dt}\theta$$

integrating : $$\int_{\theta_i}^{\theta} \frac{-\rho \cdot V \cdot C_p}{h \cdot A_s \cdot \theta}\, d\theta = \int_0^t 1\, d\tau \qquad \text{where : } \theta_i = T_i - T_{amb}$$

$$\ln\left(\frac{\theta}{\theta_i}\right) = \frac{-h \cdot A_s}{\rho \cdot V \cdot C_p} \cdot t$$

transient tmperature response : $$\frac{\theta}{\theta_i} = \exp\left(\frac{-h \cdot A_s}{\rho \cdot V \cdot C_p} \cdot t\right)$$

let : Resistance to Convective Heat Transfer : $R_t := \frac{1}{h \cdot A_s}$ $R_t = 681.708 \cdot \frac{K}{watt}$

and Lumped Thernal Capacitance : $C_t := \rho \cdot V \cdot C_p$ $C_t = 0.02 \cdot \frac{joule}{K}$

thermal time constant : $\tau_t := R_t \cdot C_t$ $\tau_t = 13.835 \cdot sec$

substituting results in : $$\frac{\theta_n}{\theta_i} = \exp\left(-\frac{t_n}{\tau_t}\right)$$

assume wire at austenite finish temperature, then : $\theta_i := T_{Af} - T_{amb}$ $\theta_i = 66.8 \cdot K$

since : $\theta = T - T_{amb}$

substituting :

temperature of wire in free convection cooling : $$T_n := T_{amb} + \theta_i \cdot \exp\left(-\frac{t_n}{R_t \cdot C_t}\right)$$

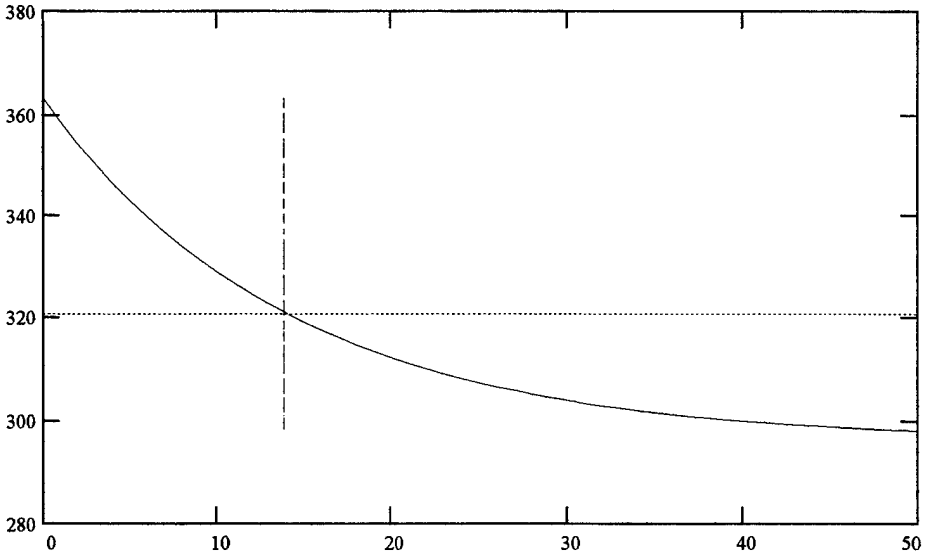

SMA Wire Temperature Response
0.368 Ti
Thermal Time Constant

Transient temperature response of SMA wire undergoing free convection cooling. Lumped capacitance method used to evaluate the transient temperature response of the SMA wire.

solving for the time required for SMA wire temperature to decay to the martensite start temperature :

$$t := -\left(R_t \cdot C_t\right) \cdot \ln\left(\frac{T_{Ms} - T_{amb}}{\theta_i}\right)$$

$$t = 2.244 \cdot \text{sec}$$

the associated energy loss :

$$E_L := (\rho \cdot V) \cdot C_p \cdot \theta_i \cdot \left(1 - \exp\left(-\frac{t}{\tau_t}\right)\right)$$

$$E_L = 0.203 \cdot \text{joule}$$

reheat time @ step current, Is :

$$\Delta t_{rh} := \frac{E_L}{I_s^2 \cdot \Omega_m \cdot La}$$

$$\Delta t_{rh} = 0.041 \cdot \text{sec}$$

Appendix A : Heat Transfer Model Calculations (continued)

Validity of Lumped Capacitance Method :

characteristic length : $L_c := \frac{V}{A_s}$ $L_c = 0.006 \cdot cm$

or more conservatively : $L_c := \frac{d}{2}$ $L_c = 0.013 \cdot cm$

Boit number : $Bi := \frac{h \cdot L_c}{k}$ $Bi = 1.764 \cdot 10^{-4}$

since Biot number is less than 0.1, the error associated with using the lumped sum capacitance method iis small

APPENDIX B. LabVIEW® PROGRAM "Wire Control & Status.vi"

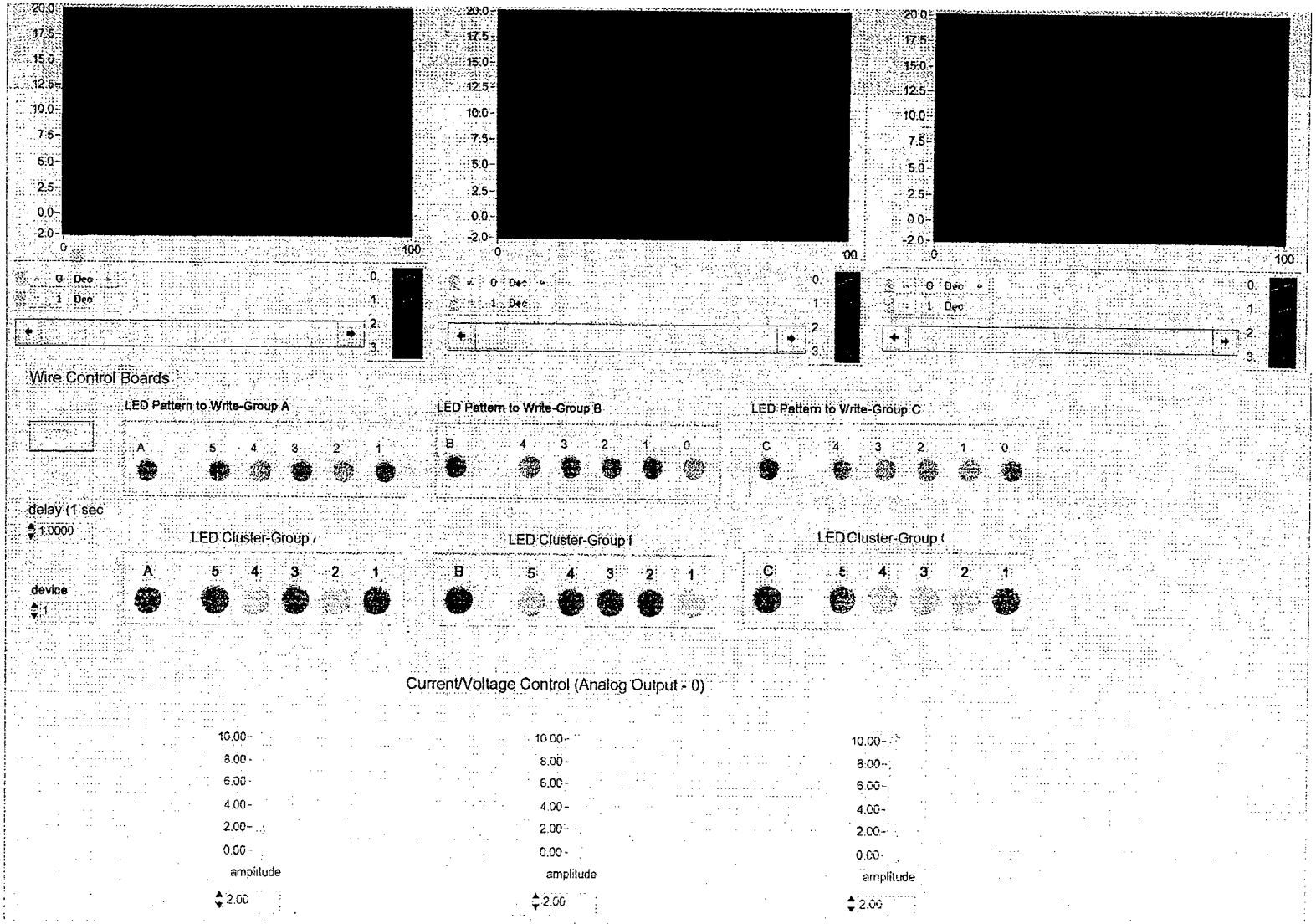
Wire Control Boards
LED Pattern to Write-Group A
LED Pattern to Write-Group B
LED Pattern to Write-Group C
delay (1 sec
1.0000
device
1
LED Cluster-Group A
LED Cluster-Group B
LED Cluster-Group C
Current/Voltage Control (Analog Output - 0)
amplitude
2.00

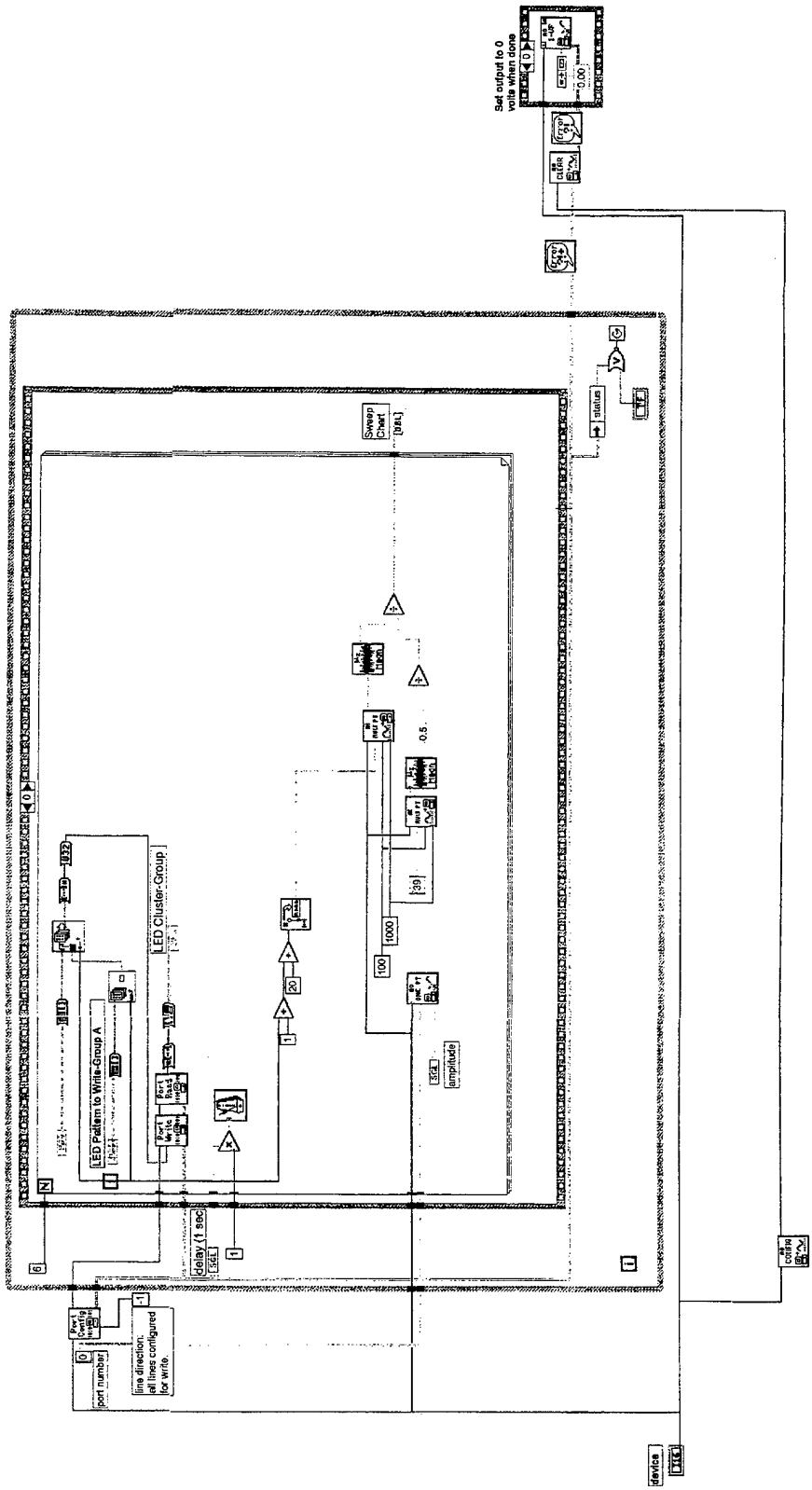
Set output to 0 volts when done
Sweep Chart
status
LED Cluster-Group
LED Pattern to Write-Group A
delay (1 sec)
port number
line direction: all lines configured for write.
amplitude
device

LIST OF REFERENCES

[1] Product Literature, Technical Characteristics of FLEXINOL™ Actuator Wires, pg i (1993).

[2] Wayman, C. M. and Duerig, T. W.; An Introduction to Martensite and Shape Memory, (Engineering Aspects of Shape Memory Alloys), (T. W. Duerig, K. N. Melton, D. Stockel, C. M. Wayman editors), Butterworth-Heinemann Ltd, Great Britain, pg 3-20 (1990).

[3] Incropera, F. P. and DeWitt, D. P.; Introduction to Heat Transfer, John Wiley & Sons, pg 9, 14-17, 226-232 (1990).

[4] Hewlett-Packard Operating Manual for the HP-6282A DC Power Supply, Table 1-1: Specifications (NPS ME Shop copy).

[5] What is MATLAB?, MATLAB® Reference Guide, The Math Works, Inc. Natick, Mass. (August 1992).

[6] Waram,T.; Design Principles For Ni-Ti Actuators, (Engineering Aspects of Shape Memory Alloys), (T. W. Duerig, K. N. Melton, D. Stockel, C. M. Wayman editors), Butterworth-Heinemann Ltd, Great Britain, pg 234-244, (1990).

[7] Melton, K. N.; Ni-Ti Based Shape Memory Alloys, (Engineering Aspects of Shape Memory Alloys), (T. W. Duerig, K. N. Melton, D. Stockel, C. M. Wayman editors), Butterworth-Heinemann Ltd, Great Britain, pg 21-35 (1990).

INITIAL DISTRIBUTION LIST

No.Copies

1. Defense Technical Information Center 2
   8725 John J. Kingman Rd., STE 0944
   Ft. Belvoir, VA 22060-6218

2. Dudley Knox Library 2
   Naval Postgraduate School
   411 Dyer Rd.
   Monterey, CA 93943-5101

3. Naval Engineering Curricular Office, Code 34 1
   Naval Postgraduate School
   700 Dyer Rd.
   Monterey, CA 93943-4004

4. R. Mukherjee 1
   Associate Professor
   Department of Mechanical Engineering
   Michigan State University
   East Lansing, MI 48824-1226

5. Prof. T. R. McNelley, Code ME/Mc 1
   Chairman
   Department of Mechanical Engineering
   Naval Postgraduate School
   700 Dyer Rd.
   Monterey, CA 93943-5100

6. LCDR Richard A. Thiel, Code 300.5 1
   Diving and Salvage Officer
   Portsmouth Naval Shipyard
   Portsmouth, NH 03804-5000